

1 **Title:** Genomic characterization of a diazotrophic microbiota associated with maize aerial root  
2 mucilage

3

4 **Author names:**

5 Shawn M. Higdon<sup>1</sup>, Tania Pozzo<sup>1</sup>, Nguyet Kong<sup>2</sup>, Bihua Huang<sup>2,3</sup>, Mai Lee Yang<sup>2</sup>, Richard  
6 Jeannotte<sup>2</sup>, C. Titus Brown<sup>2</sup>, Alan B. Bennett<sup>1\*</sup>, Bart C. Weimer<sup>2,3\*</sup>

7

8 **Affiliation:**

9 <sup>1</sup>Department of Plant Sciences, University of California, Davis, California 95616

10 <sup>2</sup>Department of Population Health and Reproduction, University of California, Davis, California

11 95616

12 <sup>3</sup>100K Pathogen Genome Project, University of California, Davis, California 95616

13 \*To whom correspondence should be sent.

14

15 Corresponding authors:

16 [abbennett@ucdavis.edu](mailto:abbennett@ucdavis.edu)

17 [bcweimer@ucdavis.edu](mailto:bcweimer@ucdavis.edu)

18

19 **Keywords:** Biological Nitrogen Fixation, Diazotrophic Bacteria, Mucilage Polysaccharide,

20 Nitrogen Fixation Gene; *Zea mays*

## 21 **Abstract**

22 A geographically isolated maize landrace cultivated on nitrogen-depleted fields without synthetic  
23 fertilizer in the Sierra Mixe region of Oaxaca, Mexico utilizes nitrogen derived from the  
24 atmosphere and develops an extensive network of mucilage-secreting aerial roots that harbors a  
25 diazotrophic microbiota. Targeting these diazotrophs, we selected nearly 600 microbes from a  
26 collection isolated from these plants and confirmed their ability to incorporate heavy nitrogen  
27 ( $^{15}\text{N}_2$ ) metabolites *in vitro*. Sequencing their genomes and conducting comparative bioinformatic  
28 analyses showed that these genomes had substantial phylogenetic diversity. We examined each  
29 diazotroph genome for the presence of *nif* genes essential to nitrogen fixation (*nifHDKENB*) and  
30 carbohydrate utilization genes relevant to the mucilage polysaccharide digestion. These analyses  
31 identified diazotrophs that possessed canonical *nif* gene operons, as well as many other operon  
32 configurations with concomitant fixation and release of >700 different  $^{15}\text{N}$  labeled metabolites.  
33 We further demonstrated that many diazotrophs possessed alternative *nif* gene operons and  
34 confirmed their genomic potential to derive chemical energy from mucilage polysaccharide to  
35 fuel nitrogen fixation. These results confirm that some diazotrophic bacteria associated with  
36 Sierra Mixe maize were capable of incorporating atmospheric nitrogen into their small molecule  
37 extracellular metabolites through multiple *nif* gene configurations while others were able to fix  
38 nitrogen without the canonical (*nifHDKENB*) genes.

39

## 40 **Data Summary**

41 Genetic resources, including biological materials and nucleic acid sequences, were accessed  
42 under an Access and Benefit Sharing (ABS) Agreement between the Sierra Mixe community and  
43 the Mars Corporation, and with authorization from the Mexican government. An internationally  
44 recognized certificate of compliance has been issued by the Mexican government under the  
45 Nagoya Protocol for such activities (ABSCH-IRCC-MX-207343-3). Any party seeking access to  
46 the nucleic acid sequences underlying the analysis reported here is subject to the full terms and  
47 obligations of the ABS agreement and the authorization from the government of Mexico.  
48 Individuals wishing to access nucleic acid sequence data for scientific research activities should  
49 contact Mars Incorporated Chief Science Officer at [CSO@effem.com](mailto:CSO@effem.com).

50

51

## 52 **Introduction**

53 Nitrogen is an essential macroelement for plant productivity that is often limiting to plant growth  
54 when the natural abundance of its bio-available forms is depleted in the environment. Exogenous  
55 nitrogen is currently provided for maize cultivation either through synthetic Haber-Bosch  
56 fertilizer produced at high environmental and economic cost (1), or from crop rotation with  
57 legumes that replenish field nitrogen levels by symbiotic association with diazotrophs, bacteria  
58 capable of biological nitrogen fixation (BNF) (2, 3). Because maize is a crop of immense  
59 agricultural importance, the establishment of conventional varieties capable of meeting their  
60 nitrogen demands through mutualistic associations with free-living diazotrophic bacteria would  
61 be of significant value to the goal of achieving global food security through sustainable  
62 intensification without relying on fertilization (4). One strategy for the discovery of useful maize  
63 diazotrophic plant-microbe associations involves exploring the microbiome of cultivated maize  
64 landraces near the center of the maize origin of domestication (5).

65         A recent report demonstrated that an indigenous landrace of maize found in Totontepec  
66 Villa de Morelos in the Sierra Mixe region of Mexico acquires 28-82% of its nitrogen from the  
67 air and exhibits an extensive system of aerial roots with heavy secretion of a mucilage composed  
68 of unique complex polysaccharides (6). Analysis of a public, low coverage shotgun metagenome  
69 sequences from the roots, stems, and aerial root mucilage revealed the aerial root mucilage  
70 microbiota to be enriched in taxa with many known species that are diazotrophic (6). In addition,  
71 the mucilage was the only plant tissue type to be enriched for homologs of the canonical nitrogen  
72 fixation genes (*nif*/HDKENB), as previously proposed by Dos Santos et al., to be essential for a  
73 bacterium to be diazotrophic (6, 7). The demonstration that the Sierra Mixe mucilage harbors a  
74 diazotrophic microbial community, that it exhibits reduced taxonomic complexity, and the

75 absence of soil from aerial root mucilage suggests that it could be a useful model system for  
76 elucidating associative mechanisms between free-living bacteria and cereal crops with mucilage-  
77 secreting aerial roots, such as maize.

78       Following investigations reported by Van Deynze et al. (6), we hypothesized that free-  
79 living diazotrophs from the aerial root mucilage microbiota utilize mucilage derived  
80 carbohydrates as an energy source for BNF. To address this, we cultured many bacteria by  
81 targeting diazotrophic bacteria specifically associated with Sierra Mixe maize. Subsequently,  
82 we characterized 588 microbial diazotrophic isolates to verify fixation and other traits using  
83 whole genome sequencing (WGS). Measuring the ability to incorporate heavy dinitrogen gas  
84 ( $^{15}\text{N}_2$ ) into secreted metabolites with tandem mass spectrometry confirmed that the isolates were  
85 diazotrophic and produced a variety of compounds containing the label. Subsequent WGS  
86 analysis using comparative genomics with each diazotrophic isolate genome included assessing  
87 differences in nucleotide composition, assigning taxonomic classifications, and estimating  
88 percent recovery from the mucilage microbiome. To elucidate the genomic determinants for  
89 BNF by mucilage-derived diazotrophs, we examined their genomes for the presence of features  
90 related to mucilage polysaccharide utilization, the canonical *nif* genes based on the Dos Santos  
91 model (7) with the *Klebsiella pneumoniae* NIF regulon as the model framework, and known  
92 alternative *nif* genes. Our results indicate that the mucilage microbial isolates contained the  
93 capacity to utilize the mucilage complex polysaccharide and, surprisingly, that many of the  
94 diazotrophic isolates did not possess recognizable homology for known *nif* genes – yet were  
95 diazotrophic. These findings suggest the presence of novel mechanisms of nitrogen fixation by  
96 many phylogenomic groups of bacteria, several of which were not previously associated with  
97 this trait.

## 98 **Methods**

### 99 **Bacterial isolation**

100 Roots, stems and mucilage (200–500  $\mu$ L) collected from different fields of the Sierra Mixe  
101 region in Mexico were spread on 1.5% BHI (BD, catalogue number 211059; Franklin Lakes, NJ,  
102 USA) or modified nitrogen-free M9 agar (BD) with and without a 1% (w/v) D-arabinose,  
103 galactose or xylose at pH 5, 5.8 or 7. Plant tissues were blended in 1 $\times$ PBS prior to culturing on  
104 medium and the blender decontaminated with 10% bleach followed by 70% ethanol between  
105 samples (v/v). Cultures were incubated at 25°C or 37°C, aerobically and anaerobically, for up to  
106 4 weeks. Once colonies appeared, they were sub-cultured on the same medium to ensure purity.  
107 Each organism was grown in BHI broth at the respective condition and resuspended in 5% non-  
108 fat dry milk and glycerol and stored cryogenically for further use.

### 109 **Biological Nitrogen Fixation Assay**

110 To assay for Microbial  $^{15}\text{N}_2$  assimilation, isolates were first grown twice overnight in the  
111 respective growth condition prior to collection and washed twice with 0.9% (w/v) saline solution  
112 before re-suspension in Fahraeus medium containing 1% D-glucose at pH 5.8 to determine the  
113 nitrogen fixation capacity. Prior to the fixation assay, dissolved oxygen was removed from the  
114 medium by sparging with argon gas for 1.5 hours while stirring and a vacuum pump was used to  
115 remove any oxygen in the headspace. Each isolate ( $\text{OD}_{600} = 2$ ; 2 mL) was added to an airtight 4  
116 mL glass vial. Addition of the heavy atom was achieved by removing 20 mL of headspace gas  
117 and replacing it with 5 mL of either  $^{15}\text{N}_2$  or  $^{14}\text{N}_2$  nitrogen gas directly into the culture. The  
118 cultures were incubated at 37 °C anaerobically for 6 - 48 hours, depending on the growth rate

119 and collected at the beginning of stationary phase for each culture. All experiments were done in  
120 triplicate.

### 121 **Microbial metabolite extraction and quantitation**

122 Subsequent to growth the metabolites were extracted from cell pellets as described by Villas-  
123 Bôas (8). Bacterial cultures were transferred to 2 mL tubes and centrifuged at 14,800 rpm for 10  
124 min at  $-9^{\circ}\text{C}$ . After collection of the cell pellet 500  $\mu\text{L}$  of cold methanol ( $-20^{\circ}\text{C}$ ) was added  
125 before lysing the cells with bead beating (9, 10). After adding 0.4 g of 0.1 mm glass beads cells  
126 were lysed by two cycles of bead beating with 30 s per cycle, 1 min rest on ice between each  
127 cycle<sup>9,10</sup>. The lysed samples were centrifuged at 14,800 rpm for 10 min at  $-9^{\circ}\text{C}$  after which 50  
128 ml of each supernatant was transferred to LC vials for metabolite analysis. Samples were stored  
129 in  $-80^{\circ}\text{C}$  until analysis using LC/TOF-MS. In order to confirm the enrichment by  $^{15}\text{N}$ , a subset  
130 of residual pellets (50 mg of dried pellets), after metabolite extraction, were submitted to the UC  
131 Davis Stable Isotope Facility for Isotope Ratio Mass Spectrometry (IRMS) analysis ( $^{15}\text{N}/^{14}\text{N}$   
132 ratio).  $^{15}\text{N}$ -labeled metabolite analysis was performed using LC-TOF G6230A (Agilent  
133 Technologies) instrument equipped with 1290 Infinity HPLC system. Chromatographic  
134 separation was performed on a Zorbax Eclipse XDB-C18 (2.1 $\times$ 15 mm, 1.8  $\mu\text{m}$ ) with a flow of  
135 500  $\mu\text{L}\cdot\text{min}^{-1}$  and the following elution gradient: 0 min, 10 % B; 2.5 min, 80 % B; 4.0 min, 100  
136 % B; 4.5 min, 100 % B; 5.0 min, 10 % B; 6.0 min, 10 %. Solvent A was water and solvent B was  
137 acetonitrile, both containing 0.1 % formic acid with a column temperature of  $40^{\circ}\text{C}$  and an  
138 injection volume of 1-5  $\mu\text{L}$ . This HPLC system was connected to an Agilent 6230 time-of-flight  
139 analyzer with an Agilent Jet Stream electrospray (ESI) interface operating in positive ion mode  
140 under the following conditions: capillary 3500 V, nebulizer 35 psi g, drying gas 8  $\text{L}\cdot\text{min}^{-1}$ , gas  
141 temperature  $350^{\circ}\text{C}$ , skimmer voltage 80 V, fragmentor voltage 135 V, octapole RF 750 V. The

142 mass axis was calibrated using the mixture provided by the manufacturer in the m/z 50–1700  
143 range. Acquisition rate was set to 1 spectrum per second (13,593 transients/spectrum). A  
144 reference solution provided continuous calibration using the following reference masses:  
145 121.0509 and 922.0098 m/z. Accurate mass spectra from 70 to 1700 m/z were recorded and  
146 processed with MassHunter Workstation software (B.04.00). Statistical analysis was performed  
147 using GeneSpring-MassProfiler Pro (version 12.1) software from Agilent Technologies, and  
148 MetaboAnalyst (<http://www.metaboanalyst.ca/>) (11).

#### 149 **Biomarkers of nitrogen-fixation**

150 The basis of this approach is that as a microbe incorporates  $^{15}\text{N}$  by fixation,  $^{15}\text{N}$  will be used in  
151 the biosynthesis of small molecules and macromolecules, such as nucleic acids and proteins,  
152 shifting their masses of 1 unit per atom of nitrogen replaced. A given bacteria fixing nitrogen and  
153 exposed to  $^{15}\text{N}_2$  gas will have a very different spectrum compared to the same bacteria exposed  
154 to  $^{14}\text{N}_2$  only.

155 The mass spectrometry analysis of each extract generated an average spectrum per  
156 sample that contains thousands of masses. All the spectra were aligned and assembled in one  
157 data matrix using SpecAlign software. Using the data from all the isolates, we performed a  
158 statistical analysis (t-test, in MetaboAnalyst) (11) to determine the features (masses) that were  
159 significantly changing across isolates when controls and treated samples were compared. This  
160 approach allows us to identify biomarkers of nitrogen fixation that could be common to all the  
161 isolates, totally or partially (some isolates could have all the biomarkers identified, some others  
162 only a subset). More than 700 masses were significantly different using a q value (a p-value  
163 adjusted by False Discovery Rate (FDR); this statistical approach allows to correct for possible  
164 false positives) of 0.05 as threshold (q value  $\leq$  0.05 was determined to be significant). Masses



165 with  $q \leq 0.05$  and fold-change (intensity of given mass in  $^{15}\text{N}$ -treated samples vs intensity of the  
166 same mass in  $^{14}\text{N}$ -treated samples) of  $>1$  were considered in the following calculations. Then for  
167 each isolate, the relative intensities (percentage of each peak raw intensity over total raw signal)  
168 for all the biomarkers were summed. Sums of the relative intensities for the biomarkers in  
169 control and treated samples, for a given isolate, were computed and ratio  $^{15}\text{N}/^{14}\text{N}$  was calculated.  
170 Isolates with BNF ratios greater than or equal to 1 were considered as sufficient  $\text{N}_2$ -fixers, where  
171 the sum of peak intensities under  $^{15}\text{N}_2$ -enriched atmosphere was found to be equal to that of the  
172 unenriched control. Following this logic, isolates with BNF ratios greater than 1 were considered  
173 to be more efficient  $\text{N}_2$ -fixers (i.e. higher  $^{15}\text{N}$  ratios indicated a higher detected abundance of  $^{15}\text{N}$   
174 atom incorporation into N-containing biomarkers) while those with ratios lower than 1 were  
175 considered low-fixing.

## 176 **Bacterial whole genome sequencing**

177 Each Sierra Mixe microbial isolate was recovered from cryogenic storage by streaking cells onto  
178 Luria-Bertani (LB) agar medium plates and incubating for one to two days at  $28^\circ\text{C}$ . Single  
179 colonies were sub-cultured in liquid LB medium at  $28^\circ\text{C}$  to an  $\text{OD}_{600}$  value of 0.7. Genomic  
180 DNA (gDNA) was extracted from the cell culture pellet of each isolate using the *Mo Bio*  
181 Ultraclean Microbial DNA extraction kit (QIAGEN, Inc). Sequencing libraries were  
182 subsequently constructed using the KAPA HyperPlus DNA library preparation kit (Roche, Inc)  
183 by following the instructions of the technical datasheet provided. A gDNA input of 100 ng was  
184 fragmented enzymatically for 9 minutes to achieve an average insert size of 450bp. The inserts  
185 were ligated to customized dual-indexed barcode adapters (Integrated DNA Technologies), and  
186 the library was size-selected by using KAPA Pure beads to carry out the kit's dual-SPRI protocol  
187 to generate an average adapter-ligated gDNA insert molecule size of 600 bp. The size-selected

188 libraries were then PCR amplified over a total of five cycles. Average library molecular size was  
189 determined using the DNA High Sensitivity Assay kit with the Agilent 2100 Bioanalyzer  
190 (Agilent Technologies). The Library was then used to generate paired end reads over 150 cycles  
191 at the UC Davis DNA Sequencing Technologies Core facility on the Illumina HiSeq 4000  
192 system.

### 193 **Isolate Genome Sequence Analysis**

194 The paired-end FASTQ files of each isolate library were quality trimmed using Trimmomatic  
195 0.36 using the following settings: ILLUMINACLIP:TruSeq3-PE.fa:2:40:15; LEADING: 2;  
196 TRAILING:2; SLIDINGWINDOW:4:15; MINLEN:50 (12). The trimmed reads were  
197 subsequently assembled using MEGAHit 1.2 with default settings (13). Assembly metrics were  
198 obtained with the default settings of QUAST 4.1, the quality assessment tool for genome  
199 assemblies (14), and the output for each assembly is summarized in S2 Table. Genome binning  
200 analysis to assess the purity of each isolate genome was carried out using the program Metabat  
201 with the default settings (15). The number of bins generated by Metabat for each isolate genome  
202 are displayed in S2 Table. Values for genomic coverage were generated by aligning trimmed  
203 reads to the resulting assemblies with BWA followed by the use of the depth function from  
204 Samtools (16, 17). Code for the Snakemake workflow used to conduct the computational  
205 analysis is available at: ([https://github.com/shigdon/snakemake\\_mucilage-isolates](https://github.com/shigdon/snakemake_mucilage-isolates)).

### 206 **Genome distance analysis and taxonomic classification**

207 Whole genome assemblies were classified and compared using Sourmash 3.1.0 (18), which  
208 provides implementation of both the MinHash and Lowest Common Ancestor (LCA) algorithms  
209 to carry out whole genome comparisons and taxonomic classification of microbial isolates in a

210 fast, efficient and lightweight computational fashion (18-20). The complete assembly files output  
211 from MEGAHit 1.2 for each isolate genome were used to generate MinHash signatures, also  
212 referred to as sketches, using the program Sourmash 3.1.0 (<https://github.com/dib-lab/sourmash>).  
213 The chosen k-mer size for each isolate genome's MinHash signature was set to 31 (k-31). These  
214 sketches served as genomic fingerprint signatures that were used to carry out an all-by-all  
215 comparison at the whole-genome level by using the 'compare' function of Sourmash to calculate  
216 Jaccard Similarity Index (JSI) values for each pairwise comparison, which was output as a  
217 matrix in csv format. This csv file was then used to generate the all by all comparative matrix  
218 and associated dendrogram in Fig. 1 using the ComplexHeatmap package in R (21). For  
219 taxonomic assignment of total genome assemblies, the k-31 signatures were queried against a  
220 database of k-31 MinHash signatures that correspond to the curated microbial genomes within  
221 the Genome Taxonomy Database (GTDB) v89 using the 'lca search' command of Sourmash  
222 (available at: <https://osf.io/wxf9z/>). K-31 MinHash signatures were also generated using  
223 Sourmash for the genome bins of each isolate genome that were created using Metabat. The  
224 MinHash signature of each genome bin was classified using the 'lca search' function of  
225 Sourmash using the aforementioned prepared database. Results from bin classification using  
226 Sourmash are presented in S4 Table. Quantification of full taxonomies generated using  
227 Sourmash LCA classification data from isolate genome bins derived was visualized as a Heat  
228 Tree using Metacoder 0.3.1 in R (22). Code used to generate, compare and classify MinHash  
229 genome sketches is included in the Snakemake workflow hosted at:  
230 ([https://github.com/shigdon/snakemake\\_mucilage-isolates](https://github.com/shigdon/snakemake_mucilage-isolates)). Code used for analysis of Sourmash  
231 output and figure generation in R is available at: ([https://github.com/shigdon/R-Mucilage-](https://github.com/shigdon/R-Mucilage-isolates-sourmash)  
232 [isolates-sourmash](https://github.com/shigdon/R-Mucilage-isolates-sourmash)).

## 233 **Mucilage metagenome taxonomic classification**

234 Paired end Illumina sequence data from Sierra Mixe aerial root mucilage metagenome sample  
235 OLMM00 was downloaded from Figshare  
236 (<https://figshare.com/s/04997ae7f7d18b53174a#/articles/6615497>) and analyzed to characterize  
237 the breadth of microbial diversity present within the mucilage environment. The shotgun  
238 metagenomic reads were quality filtered using Trimmomatic 0.36 and the surviving reads were  
239 separated into microbial and non-microbial fractions using the classify function of Kraken2  
240 2.0.8\_beta with the Refseq complete databases for Bacteria, Archaea, and Viruses (23, 24). The  
241 microbial component of OLMM00 classified with Kraken2 was subsequently visualized using  
242 the R package MetacodeR at the Phylum, Class, Order and Family levels, which is presented in  
243 Fig S1 (25). The relative abundance of each microbial taxon classified at the genus level was  
244 computed after performing Bayesian re-estimation of hits using Bracken2 (26) and normalization  
245 of read classifications for each taxon with the counts per million method using the R package  
246 Phyloseq (S6 Table) (27). Prior to analyzing the microbial community, the table of classified  
247 microbial taxa output by Bracken2 was filtered to remove taxa for which the number of  
248 classified reads was below 500, which resulted in a total of 609 unique genera identified within  
249 the OLMM00 metagenome (S7 Table). Source code for analysis and figure generation is  
250 available at: (<https://github.com/shigdon/R-Mucilage-Metagenome>).

## 251 ***Nif* and alternative *nif* gene mining**

252 Protein coding sequences were predicted for each microbial isolate genome by using the  
253 corresponding MEGAHit-assembled contigs as input files for the prokaryotic genome annotation  
254 program Prokka 1.12 (28). The multi-FASTA amino acid files output for each isolate genome

255 were scanned against profile hidden markov models (pHMMs) corresponding to *nif* genes of the  
256 *K. pneumoniae* NIF regulon using the ‘hmmScan’ function of HMMER 3.1b (29). These were  
257 acquired from the Pfam and TIGRFAM libraries of pHMMs (30, 31). HMM hits for each *nif*  
258 gene were stringently filtered in R using the dplyr package to retain query-subject hits that  
259 maintained model coverage greater than or equal to 75 % and a maximum e-value of  $1e^{-9}$  (32).  
260 Visualization of *nif* gene profiles for all pure isolates depicted in Fig 3 was achieved using the  
261 Complex Heatmap package in R by clustering pure isolates based their relative MinHash  
262 distances and displaying counts of unique coding sequences that were found to match each *nif*  
263 HMM (21). TIGRFAMs used to scan for canonical *nif* genes of the *K. pneumoniae* NIF regulon  
264 included: TIGR01817, TIGR02938, TIGR02176, TIGR01287, TIGR01282, TIGR01286,  
265 TIGR01283, TIGR01285, TIGR01290, TIGR02000 TIGR03402, TIGR02660, TIGR02933 and  
266 TIGR01752. Pfams used to scan for *nif* gene mining included: PF04891.11 and PF03206.13.  
267 TIGRFAMs used to scan for alternative *nif* gene mining included: TIGR01860, TIGR02930,  
268 TIGR02932, TIGR01861, TIGR02929 and TIGR02931. The corresponding hmmScan results for  
269 alternative *nif* genes were filtered to retain query-model matches with maximum e-values of  $1e^{-06}$   
270 and 85 % minimum model coverage. Source code for bacterial genome mining analyses and  
271 figure generation is available at: (<https://github.com/shigdon/R-Mucilage-isolates-nif>) and  
272 (<https://github.com/shigdon/R-alt-nif-analysis>).

### 273 **CAZyme gene mining**

274 The multi-FASTA amino acid files for each microbial isolate genome that were generated by  
275 Prokka were each used as input for the dbCAN2 analytical pipeline (33). This was achieved  
276 using a local installation of the source code for the dbCAN2 pipeline hosted on Github  
277 ([https://github.com/linnabrown/run\\_dbcan](https://github.com/linnabrown/run_dbcan)). Output files in CSV format were read into R and

278 filtered using the R packages within tidyverse 1.2.1 (34). Circular heatmap plots were made  
279 using the ggtree package (35). Source code for analysis and figure generation is available at:  
280 (<https://github.com/shigdon/R-Mucilage-isolates-dbCAN2>).

## 281 **Pan-genome Analysis**

282 Genomic features predicted by Prokka (36) for each microbial genome included in the isolate  
283 sub-population study were aggregated in GenBank feature format and collectively used as input  
284 for pan-genome analysis using the program Roary 3.12.0 (37). Configuration for running the  
285 Roary microbial pan-genomic pipeline included use of the “-e” flag to generate a multi-FASTA  
286 alignment of core genes using PRANK and a minimum blastp identity value of 95 percent. To  
287 visualize the pan-genome of the isolate set presented in Fig 5C, the gene presence and absence  
288 output file, the associated dendrogram and an isolate-genus mapping file were uploaded to the  
289 Phandango web server (38). Source code for analysis and figure generation is available at:  
290 (<https://github.com/shigdon/R-alt-nif-analysis>).

## 291 **Results**

### 292 **Diazotrophic isolates were confirmed by functional assay of $^{15}\text{N}_2$ incorporation**

293 We isolated putative diazotrophic bacteria in samples collected from Sierra Mixe maize plants  
294 grown using a nitrogen-deficient basal medium supplemented with sugars corresponding to the  
295 monosaccharide composition of aerial root mucilage (S1 Table). Culturing each isolate in N-  
296 deficient liquid media under an atmosphere containing  $^{15}\text{N}_2$  gas and measuring their ability to  
297 incorporate  $^{15}\text{N}$  atoms into small molecule metabolites ( i.e. <1000 Da) by Time of Flight mass  
298 spectrometry confirmed that the isolates were diazotrophic and produced a large number of

299 compounds with different masses and chemical structures. Summation of peak intensities for N-  
300 containing compounds common to enriched and control (compressed air) cultures enabled each  
301 isolate's BNF capacity to be measured as a ratio of  $^{15}\text{N}/^{14}\text{N}$  (BNF ratio). Overall, BNF ratios  
302 obtained for all pure isolates assayed ranged from 0.6 to 4.6 (Table S2). While most isolates  
303 exhibited moderate BNF ratios between 1 and 2, ~5% of the isolates demonstrated N-fixation  
304 with BNF ratios  $>2$  (Table 1). The observed BNF ratio variation among these confirmed  
305 diazotrophs prompted investigation of the underlying genomic determinants for BNF of each  
306 isolate.

### 307 **Whole genome analysis revealed significant phylogenetic diversity**

308 The selected bacterial isolates were subjected to WGS and resulted in a collection of draft  
309 genome assemblies with fold coverages that ranged from 14 – 330X (S3 Table). Analysis of  
310 mucilage isolates revealed an unexpected range of diversity in nucleotide composition and  
311 taxonomy. All-by-all comparison of MinHash sketches for each isolate genome depicted the  
312 relative genomic distances of all pairings that verified the diversity of genomes (Fig 1).  
313 Complete taxonomic classification for each bacterial genome (S4 Table) at the maximum sketch  
314 size found 33 known bacterial taxa among the 472 isolate genomes, and 116 genomes that were  
315 unidentified (Fig 1). Possible explanations for unidentified isolates included lack of a database  
316 accession match or the presence of multiple bacterial genomes within a WGS MinHash sketch  
317 that triggered disagreement within the genomic classification structure of the lowest common  
318 ancestor algorithm (LCA).

319 To assess whether isolate genomes were pure or derived from a mixed culture that  
320 appeared pure during isolation, we used Metabat (15) to bin each WGS assembly and identify  
321 isolates comprised of multiple organisms. This resulted in 492 isolate genomes with single bins

322 of single organism DNA sequences (Fig 1, S6 Table) – indicating pure cultures. WGS assemblies  
323 with 2, 3, 4 and 5 bins had frequencies of 72, 19, 3 and 2, respectively (Fig 1 and S3 Table),  
324 indicating that what appeared to be a single colony contained multiple organisms and that further  
325 WGS analysis was needed to deconvolute respective sequences. Reexamination of the  
326 deconvoluted genomes for taxonomic classification of each genome bin increased the resolution  
327 of microbial diversity and augmented the diversity of the taxa present and capable of fixing  
328 nitrogen (S5 Table).

329 Visualization of the classified genome bins indicated that the selected isolates were  
330 primarily comprised of Proteobacteria, a substantial number of Firmicutes, and relatively few  
331 Actinobacteria (S1 Fig). While deconvoluted genomes largely classified as  
332 Gammaproteobacteria, relatively few deconvoluted genomes were classified to the  
333 Alphaproteobacteria or Betaproteobacteria classes. Congruent with the findings of Carvalho et  
334 al., several deconvoluted genomes from our study were classified as *Burkholderia*, along with  
335 other Betaproteobacteria that included *Achromobacter*, *Acidovorax* and *Herbaspirillum* (39).  
336 However, deconvoluted genomes classified as *Enterobacter*, *Klebsiella*, *Metakosakonia*,  
337 *Rahnella*, *Raoultella*, and *Pseudomonas* were among the most abundant in the mixed cultures.  
338 Membership of deconvoluted genomes classified to Firmicutes included a substantial number of  
339 *Lactococcus* and several were identified as *Enterococcus* and *Bacillus*. Included in the few  
340 Actinobacteria genomes sequenced, deconvoluted genome analysis found *Curtobacterium*,  
341 *Leifsonia*, *Microbacterium*, *Micrococcus* and *Rhodococcus* as well.

342 Comparison of the deconvoluted genomes and pure genomes for taxonomic content with  
343 the OLM00 mucilage metagenome reported by Van Deynze et al. (6) indicated that the  
344 culturing strategy enriched the isolates that fixed nitrogen and obtained a small fraction of the



345 possible mucilage microbiome reported from the low sequence coverage metagenome. Using  
346 609 genera identified in OLMM00 as a benchmark for bacterial diversity (S7 Table), the unique  
347 genera classified among isolate WGS assemblies comprised ~5% of genera in the mucilage  
348 microbiome. In addition, analysis of OLMM00 metagenome provided further insight to the  
349 phylogenetic diversity of mucilage microbiota associated with this landrace (S8 Table).  
350 Proteobacteria, Bacteroidetes, Actinobacteria and Firmicutes were the most abundant phyla in  
351 the mucilage microbiome (S2 Fig, S8 Table). However, confirmation of multiple organisms  
352 contributing to mixed cultures (i.e. composite genomes) limited our ability to attribute observed  
353 BNF phenotypes to a distinct organism within co-cultured isolates. This observation prompted  
354 genomic profiling of each pure isolate genome for carbohydrate utilization and *nif* features to  
355 address the hypothesis that mucilage diazotrophs derive energy from mucilage polysaccharide to  
356 fuel BNF.

357 **Diazotrophic isolates possessed CAZymes and sugar transporters relevant for mucilage**  
358 **digestion**

359 Examining isolate genomes for glycosyl hydrolase (GH) genes relevant to the composition of  
360 aerial root mucilage polysaccharide (6, 40) was done using Hidden Markov Models (HMMs) of  
361 GH families in the Carbohydrate Active Enzymes (CAZy) database (S9 Table) (41). This  
362 analysis revealed that the pure culture diazotrophs contained genes supporting the genomic  
363 potential to degrade and derive energy from mucilage polysaccharides. Targeting GHs with  
364 arabinofuranosidase, fucosidase, galactosidase, glucuronidase, mannosidase and xylosidase  
365 activities revealed that diazotrophic genomes with small differences in genome diversity  
366 contained similar GH profiles spanning 12 functional GH groups (Fig 2A). Comparison of GH  
367 groups conferring arabinofuranosidase and/or xylosidase activities demonstrated that the more

368 promiscuous ‘Ara/Xyl’ GH group had the highest abundance with increased genome copy  
369 number for the majority of classified genomes. GH groups with exclusive galactose or mannose  
370 substrate specificities were also abundant in the isolates examined, where the sum of the isolates  
371 with genes in these GH groups was determined to be 366 of the 492 genomes (S10 Table). In  
372 contrast to the plethora of genomes found to possess pentose and/or hexose cleaving GHs, those  
373 with strict glucuronate and fucose specificities were far less abundant in the pure cultures.  
374 Interestingly, most genomes possessed genes in GH groups with promiscuous substrate  
375 specificities that encompassed the complete range of mucilage polysaccharide compositional  
376 diversity across five different GH families (GH1, GH2, GH31, GH4, GH30).

377         In addition to generating GH profiles, querying genomes for the presence of sugar  
378 transport genes relevant to monosaccharides that contribute to mucilage polysaccharide structure  
379 revealed that isolated diazotrophs possess the machinery necessary for transport of mucilage-  
380 derived monosaccharides obtained from the digestion of mucilage, indicating that the initiating  
381 step of catabolism was present in the genome (Fig 2B). Utilizing a list of mucilage relevant  
382 accessions (S11 Table) from the Transporter Classification Database (TCDB) (42), we generated  
383 sugar transport profiles for each genome. Summarizing genome counts by genus level  
384 classification demonstrated that those classified to the most common Gammaproteobacteria  
385 exhibited sugar transporters for all six monosaccharide moieties derived from the mucilage  
386 polysaccharide (S12 Table). Additionally, isolates of the most commonly classified genera  
387 possessed multiple genes and/or mechanisms for transport of each monosaccharide type in  
388 mucilage. Genomes assigned to less abundant genera tended to exhibit higher variation in sugar  
389 transporter profiles, where the absence of known carbohydrate transport systems corresponding  
390 to some, but not all components of mucilage polysaccharide was observed. This observation may

391 explain how the culturing strategy resulted in reflecting abundant members of the mucilage  
392 microbiome.

### 393 **Diazotrophic isolates displayed genomic variation in canonical *nif* gene features**

394 The genetic basis for BNF was established following more than 100 years of research, where  
395 numerous *nif* genes have been implicated as contributing factors to the phenotype with various  
396 operon configurations (43). We investigated the genomic mechanism for the diazotrophic  
397 phenotype (i.e. BNF) by examining the predicted coding sequences using HMMs for the six *nif*  
398 genes of the Dos Santos model (7) within the context of seven genetic operons comprising the  
399 *K. pneumoniae* NIF regulon, which included: 1) the operon of *nif* genes involved in regulation of  
400 the *nif* pathway, *nifRLA*; 2) the catalytic operon, *nifHDK*; 3) operons involved in formation of  
401 the functional Fe-Mo protein, *nifEN* and *nifBQ*; 4) an operon of genes involved in assembly of  
402 the functional enzyme complex, *nifUSVM*; and 4) operons conferring genes associated with  
403 mediating electron transfer, *nifJ* and *nifWF* (44, 45). Results from this extensive analysis  
404 generated *nif* gene profiles and revealed three distinct groups of diazotrophic isolates (NIF  
405 groups) based on *nif* gene content and variation in structure (Fig 3). NIF groups included a subset  
406 of 193 genomes positive for the presence of homologous protein-coding sequences to HMMs for  
407 all *nif* genes in the Dos Santos model (DS-positive, DSP), a smaller subset of 66 isolates with *nif*  
408 gene profiles reflecting a semi-complete set of Dos Santos model *nif* genes (Semi-DS, SDS) and  
409 a subset of 233 isolates that completely lacked genes with HMM homology for all Dos Santos  
410 model *nif* genes (DS-negative, DSN), yet phenotypically displayed diazotrophy.

411 Although each NIF group included genomes classified from a range of bacterial genera,  
412 each group also included diazotrophs with an “unassigned” taxonomic classification (S6 Table).  
413 However, DSP genomes positively classified to known genera were comprised entirely of

414 Gammaproteobacteria assigned to *Enterobacter*, *Klebsiella*, *Kosakonia*, *Metakosakonia*,  
415 *Pseudomonas*, *Rahnella* or *Raoultella*. SDS isolates had much higher taxonomic diversity, where  
416 SDS group membership was attributed by pure isolates from Actinobacteria, Firmicutes and  
417 Proteobacteria. Within these three phyla, SDS isolate genera included *Acidovorax*,  
418 *Acinetobacter*, *Bacillus*, *Curtobacterium*, *Herbaspirillum*, *Leifonia*, *Micrococcus*, *Pseudomonas*  
419 and *Stenotrophomonas*. In a fashion similar to SDS isolates, DSN genomes were also composed  
420 of Actinobacteria, Firmicutes and Proteobacteria. Interestingly, DSN genomes displayed the  
421 highest taxonomic diversity among the three NIF groups by including *Acinetobacter*,  
422 *Agrobacterium*, *Atlantibacter*, *Citrobacter*, *Curtobacterium*, *Enterobacter*, *Erwinia*, *Escherichia*,  
423 *Hafnia*, *Lactococcus*, *Lelliottia*, *Metakosakonia*, *Microbacterium*, *Morganella*, *Pantoea*,  
424 *Pseudomonas*, *Rahnella*, *Rhodococcus*, *Serratia* and *Staphylococcus*. While genomes classified  
425 as *Enterobacter*, *Metakosakonia* and *Rahnella* were found in both the DSP and DSN groups,  
426 *Pseudomonas* genomes were present in all three NIF groups. In addition to *Pseudomonas*,  
427 commonalities between genera identified within the SDS and DSN groups included membership  
428 to *Acinetobacter* and *Curtobacterium*.

429       Every genome from a diazotroph in the DSP group possessed homologous protein coding  
430 regions to *nif* genes in the *K. pneumoniae* NIF regulon (Fig 3, S3 Fig). Importantly, diazotrophs  
431 in this group possessed homologs to the six *nif* genes of the Dos Santos Model and exhibited  
432 BNF ratios that confirmed their ability to fix atmospheric nitrogen. The majority of diazotrophs  
433 in the DSP group had moderate BNF ratio values within the inclusive range of 1 to 2, and four  
434 isolates exhibited capacity ratios > 2 (Fig 4A). While the 21 *Rahnella* genomes were the only  
435 subset found to possess homologs for all 16 *nif* genes investigated, the remaining 172 genomes  
436 lacked homologs to either the *nifJ*, *nifL*, *nifQ* or *nifW* genes in variable degrees and/or

437 combinations. However, these diazotrophs exhibited nearly identical *nif* gene profile  
438 compositions with the exception of slight variations in gene copy number. In the case of DSP  
439 isolates classified as *Enterobacteriaceae*, distinguished clades of *Enterobacter* and *Klebsiella*  
440 genomes each lacked homologous genes to *nifL* and *nifW* while clades of *Pseudomonas* and  
441 most *Rahnella* genomes were the only diazotrophs with homologs for the *nifW* gene. With  
442 respect to the *nifH* gene encoding the dinitrogenase reductase protein, 150 genomes in the DSP  
443 category had single copy homologs and 43 exhibited the presence of two copies. Overall, the *nif*  
444 gene content and BNF ratios of diazotrophs in the DSP group demonstrated that many mucilage  
445 diazotrophs adhered to the *K. pneumoniae* NIF regulon and Dos Santos models to conduct BNF.

446 All 66 members of the SDS group contained homologs to at least one, but not all, of the  
447 essential *nif* genes in the Dos Santos model (Fig 3, S4 Fig) and fixed nitrogen with BNF ratios  
448 similar to diazotrophs in the DSP group (Fig 4B). In a similar fashion to the DSP isolates, all  
449 SDS isolates were found to possess homologs for at least one copy of the *nifH* gene but  
450 interestingly two copies were detected in 15 diazotrophs of the SDS group. Genes homologous to  
451 dinitrogenase component I, *nifD* and *nifK*, were only found in a single isolate of the SDS group.  
452 Regarding the three *nif* genes involved with biosynthesis of FeMoCo, only a single SDS isolate  
453 (BCW-200147) possessed homologs to *nifE* and *nifN*, and genes matching the HMM for *nifB*  
454 were not detected in any SDS diazotroph genomes. Beyond Dos Santos' model of essential *nif*  
455 genes, many SDS isolates possessed homologs for several genes in the *nifRLA* and *nifUSVM*  
456 operons of *K. pneumoniae*, but genes involved with electron transfer (*nifF* and *nifJ*) were not  
457 detected among the majority of isolates in this group. Despite lacking the complete set of *nif*  
458 genes in the Dos Santos Model, BNF ratios for isolates in this group ranged from 0.8 to 3.0.  
459 Taken together, *nif* gene analysis combined with the diazotrophic phenotype (i.e. BNF ratios) in

460 the SDS group revealed that many mucilage isolates exhibited BNF activity without the presence  
461 of any essential *nif* genes defined by the Dos Santos model, suggesting that a novel mechanism  
462 of diazotrophy may be expressed in the microbiome of this landrace.

463 Contrary to the DSP and SDS NIF groups, the 233 diazotrophs in the DSN group  
464 completely lacked the presence of homologous protein coding sequences for all *nif* genes in the  
465 Dos Santos model (Fig 3, S5 Fig) and exhibited BNF ratios that rivaled those of diazotrophs in  
466 the other NIF groups containing gene matches to HMMs for all or part of the *nif* genes in the Dos  
467 Santos model (Fig 4C). Members of the DSN group lacked homologs for many *nif* genes  
468 constituting the NIF regulon of *K. pneumoniae*, and nearly all of them possessed coding  
469 sequences resembling genes of the *nif*USVM operon. While many DSN genomes encoded  
470 homologous genes to the BNF regulatory protein *nifA*, members of this group contained gene  
471 sequences that matched the *nifL* HMM to a much lesser extent. Contrary to the observed *nif* gene  
472 profiles of diazotrophs in the SDS group, observed trends for DSN genomes included presence  
473 of homologous sequences to the *nifF* and *nifJ* genes involved with electron transfer. Similar to  
474 observations made with the other two NIF Groups, 188 DSN diazotrophs exhibited BNF ratios  
475 between 1 and 2. Surprisingly, among all three NIF Groups, the DSN group presented the largest  
476 number of diazotrophs with BNF ratio values > 2. Collectively, *nif* gene profiles of DSN  
477 genomes and their corresponding BNF assay results demonstrated that these diazotrophs were  
478 capable of BNF without employment of any *nif* genes in the Dos Santos model and only a subset  
479 of the *K. pneumoniae* NIF regulon.

#### 480 **Alternative *nif* genes were detected in isolates with substantial genome variation**

481 Following queries for canonical *nif* genes of the Dos Santos model, we investigated whether the  
482 bacterial genomes encoded *nif* genes for known alternative nitrogenase systems that either

483 strictly utilize iron (*anf*) or incorporate vanadium in place of molybdenum (*vnf*) as metal co-  
484 factors of dinitrogenase (43). Utilizing TIGRFAMs for the *anfD*, *anfK*, *anfG*, *vnfD*, *vnfK* and  
485 *vnfG* nitrogenase genes along with those of the Mo-Fe type nitrogenase (*nifHDK*), HMM  
486 analysis of predicted protein sequences from each genome revealed a small subset of diazotrophs  
487 with alternative *nif* genes. This resulted in the identification of 42 genomes with coding  
488 sequences that matched all nine *nif* HMMs (Fig 5A). Investigation of these *nif* genes also  
489 confirmed 146 diazotrophs in possession of the *nifHDK* operon without genes matching  
490 alternative nitrogenase HMMs, and 63 that had genes matching only the HMM model for *nifH*.  
491 Investigating the genomes with alternative *nif* genes revealed that each was previously assigned  
492 to the DSP group. This observation warranted further investigation of genomic similarities and  
493 differences between the 42 genomes with alternative *nif* genes.

494 WGS comparison of diazotrophs that contained alternative *nif* genes uncovered  
495 substantial phylogenomic diversity within the group. Computation of genomic distances between  
496 the 42 previously identified genomes revealed 12 distinct groupings of highly similar diazotrophs  
497 with JSI of nearly 1 (Fig 5B). Cross-referencing previously generated taxonomy for these  
498 alternative *nif*-possessing diazotrophs revealed two genera classifications. Among these  
499 taxonomic assignments, 38 isolates were classified to be *Raoultella*, 2 isolates were classified as  
500 *Metakosakonia*, and 2 were classified as *Enterobacteriaceae*. This indicated that the majority of  
501 diazotrophs with homologs to alternative *nif* genes had genomes with significant nucleotide  
502 similarity to reference genomes in the Genome Taxonomy Database (GTDB) classified as  
503 *Raoultella* (46). Interestingly, diazotrophs classified as *Raoultella* exhibited broad genomic  
504 diversity and formed multiple taxonomic clusters, with the two “unassigned” genomes  
505 interspersed among them, suggesting that they are near relatives of *Raoultella*. Comparison of



506 the JSI values between genomes classified as *Raoultella* presented values ranging from 0.1 to 1.  
507 Additionally, the two *Metakosakonia* genomes presented strong dissimilarity to the other 40  
508 isolates with JSI values close to zero for each pairing. These observations indicated large  
509 variation in genome composition for this subset of isolated diazotrophs and prompted subsequent  
510 exploration of the pan-genome among isolates that lack classical *nif* genome construction yet fix  
511 nitrogen.

512 Observed differences in nucleotide composition among genomes with alternative *nif*  
513 genes were expanded by elucidating the pan-genome for this group of diazotrophs. Annotated  
514 protein coding features of each genome served as inputs for pan-genome analysis to determine  
515 the core genome among diazotrophic isolates with alternative *nif* genes (37). Pan-genome  
516 analysis revealed a narrow core genome comprised by 285 of the 15,353 genes provided as input  
517 (S13 Table) with 3,374 soft core genes, 2,532 shell genes and 9,162 cloud genes occurring  
518 within 95 – 99, 15 – 95, and 0 – 15 % of diazotrophic genomes, respectively. Genome clustering  
519 based on the presence and absence of annotated genomic features (Fig 5C) was highly similar to  
520 that observed using MinHash, where the isolate groupings of the phylogenetic tree generated  
521 using the pan-genome corresponded with clades determined using genome distance differences  
522 (Fig 5B). Although taxonomic annotation of diazotrophs comprising the pan-genome suggested  
523 many distinct groups of *Raoultella* genomes (annotated in green), interspersed among the two  
524 “unassigned” genomes with small blocks of unique coding features (annotated in purple) among  
525 the defined clades of *Raoultella* corroborated findings from the MinHash analysis with blocks of  
526 core genes. Visualization of the pan-genome revealed the *Metakosakonia* clade (annotated in  
527 orange) of two diazotrophs (BCW201058 and BCW201155) as a near relative to the duo of  
528 distinguished *Raoultella* genomes (BCW200600 and BCW201900), which confirmed findings



529 from the genome distance analysis. Furthermore, these four genomes possessed large blocks of  
530 features absent from the other 38 genomes in the group.

## 531 **Discussion**

### 532 **Diazotrophic isolates represented a small fraction of the mucilage microbiome**

533 The strategy to isolate diazotrophs focused on simulating the native environment of aerial root  
534 mucilage (anaerobic/microaerophilic, pH and temperature) in combination with nitrogen  
535 deprivation. This enabled providing various carbon sources associated with the mucilage  
536 polysaccharide to force expression of the metabolic traits that are likely associated with growth  
537 and survival on maize during *in vitro* isolation and selection (S1 Table). This was based on the  
538 two-component hypothesis that diazotrophs of the resident microbiota incorporate atmospheric  
539 nitrogen into various compounds via BNF, which is biologically powered by ATP when utilizing  
540 sugars derived from mucilage polysaccharides to fuel the energy needs of the energetically  
541 expensive transformation. Successful generation of a large isolate collection from mucilage with  
542 this strategy set the stage for further investigations to confirm the putative diazotrophic isolates.  
543 In response, this study established an *in vitro* functional metabolomic assay to quantify each  
544 isolate's ability to incorporate heavy nitrogen into various extracellular metabolites, which both  
545 confirmed the diazotrophic nature of isolates in this collection and verified the efficacy of the  
546 strategy to recover diazotrophs (Table 1, Fig 4, S2 Table).

547 WGS of nearly 600 diazotrophic isolates provided a means to assess the taxonomic  
548 diversity of the isolate collection relative to that of the mucilage microbiome. Concerns of isolate  
549 misclassification were avoided by using whole genome analysis and composition to assign  
550 taxonomy for diazotrophic genomes rather than a conserved marker gene with higher sequence

551 conservation (47, 48). Utilizing Kraken to classify genera derived from normalized read counts  
552 (49) of the previously reported OLMM00 mucilage metagenome (6) (S7 Table, S8 Table)  
553 identified 609 genera, of which the diazotrophic genome collection had 29 in common (S5  
554 Table). This revealed ~5% of the bacterial diversity from the aerial root mucilage microbiota is  
555 contained within the isolate collection and demonstrated that the cultured subpopulation had 25%  
556 of the top 20 most abundant known genera in the OLMM00 metagenome. Although many  
557 diazotroph genomes were “unassigned” taxonomically, which highlights the potential novelty of  
558 many bacteria in this isolate collection, metagenome sequencing of mucilage samples at a higher  
559 depth and re-classification of isolate genomes following expansion of microbial WGS databases  
560 should be achieved in the future to verify these results.

561 Comparing taxa classified in the mucilage metagenome to taxonomically classified  
562 diazotroph genomes validated our strategy to recover taxa with both high relative abundance in  
563 the aerial root mucilage microbiome and functionally important traits. Notably, the majority of  
564 genomes in our collection were classified to the Actinobacteria, Firmicutes, and Proteobacteria  
565 phyla, which strongly aligns with previous efforts to characterize plant-associated microbiomes  
566 (S1 Fig, S4 Table) (50-52). Reads classified to *Pseudomonas* in OLMM00 had the highest relative  
567 abundance among genera in the metagenome, and this isolate collection contained several  
568 distinct clades of *Pseudomonas* based on the substantial genome dissimilarity observed from all-  
569 by-all whole genome sequence comparisons (Fig 1). Whole genome taxonomic classification of  
570 diazotroph genomes also revealed presence of the second most abundant genus of OLMM00,  
571 *Acidovorax*, in the collection, as well as others assigned to genera with high relative abundance  
572 in the mucilage metagenome that include *Agrobacterium*, *Herbaspirillum* and *Burkholderia*.  
573 However, the majority of classified diazotrophs were Gammaproteobacteria that exhibited low

574 relative abundance in OLMM00 (S1 Fig, S2 Fig, S7 Table). This suggested that diazotrophic  
575 contributions to Sierra Mixe maize by the mucilage microbiome may originate from community  
576 members of lower abundance, as evidenced by the diverse set of diazotrophic isolates described  
577 here. Furthermore, comparison of taxonomic analysis between whole genome sequences of  
578 selected diazotrophs and the OLMM00 metagenome suggested that microbial diversity of the  
579 mucilage microbiome is much broader than that of the collection. This suggests that diazotrophy  
580 may not be a widespread feature among genera detected in the OLMM00 mucilage metagenome.

### 581 **Diazotrophs exhibited the genomic potential for mucilage polysaccharide utilization**

582 Utilizing the canonical pathway for BNF, one of the most energy-intensive biochemical  
583 processes in biology that consumes 16 ATP per reaction cycle to convert a single dinitrogen  
584 molecule into ammonia (53), an actively fixing diazotroph associated with Sierra Mixe maize  
585 would require a reliable feedstock to produce chemical energy. Based on the diverse  
586 monosaccharide composition (arabinose, fucose, galactose, glucuronate, mannose, xylose) of  
587 aerial root mucilage polysaccharide (6, 54) and evidence of endogenous GH activity present in  
588 fresh mucilage samples (55), we surmised that harnessing it for energy to drive BNF requires  
589 bacterial genes encoding both GHs to facilitate polysaccharide catabolism, and those conferring  
590 the ability to transport smaller sugars into the cell. We mined isolate genomes for carbohydrate  
591 utilization genes and parsed relevant data using manually curated lists of relevant database  
592 accessions (S9 Table and S11 Table) (33).

593 GHs are the most abundant class of carbohydrate active enzymes (CAZymes) and consist  
594 of over 150 distinct families with documented substrate specificities (56). Importantly, GHs  
595 often attribute multiple substrate specificities while maintaining similar protein domain  
596 architectures and sequence similarity. This ascribes the potential for substrate promiscuity among

597 GH enzymes classified to a given GH family based on differences in protein structure. The GH  
598 profiles of isolate genomes indicated that mucilage diazotrophs possess the genomic potential to  
599 liberate monosaccharide components of the mucilage polysaccharide (Fig 2A). A summary of  
600 diazotrophic isolate counts for the number of isolates with genes in each GH group by genus  
601 classification further suggested that the majority of isolated diazotroph genomes encode highly  
602 specific as well as promiscuous GHs (S10 Table). These results indicated that mucilage  
603 diazotrophs are capable of liberating multiple polysaccharide derivatives irrespective of  
604 taxonomic assignment.

605         While the ability to liberate small carbohydrates from mucilage polysaccharide is  
606 necessary for its utilization as an energy source, diazotrophs from this niche must also possess  
607 the corresponding sugar transport systems. Bacteria possess multiple mechanisms for  
608 monosaccharide transport that primarily consist of membrane bound permeases, symporters,  
609 ABC-type porters and phosphotransferase (PTS) systems (57). We found the presence of sugar  
610 transporters from these classes with specificities for all six monosaccharide derivatives of  
611 mucilage polysaccharide in all of the genomes (Fig 2B, S12). Considering these findings along  
612 with observations that mucilage diazotrophs possessed highly promiscuous GHs corresponding  
613 to the mucilage composition, we surmised that mucilage bacteria are theoretically capable of  
614 utilizing their endogenous carbohydrate utilization genes to derive energy from mucilage  
615 carbohydrates. Broadly, this analysis confirmed that the majority of our diazotrophic isolates  
616 possess genes that may confer the ability to derive energy from mucilage polysaccharide and  
617 provides additional support for the hypothesis that diazotrophs of the mucilage microbiota utilize  
618 the polysaccharide to drive BNF.

619 **Diazotrophs formed three distinct nitrogen fixation groups based on genome analysis.**

620 Based on the isolation strategy to enrich for diazotrophic bacteria from the mucilage microbiome  
621 and the confirmed BNF phenotypes of diazotrophic isolates, we hypothesized that the  
622 diazotrophic genomes contain the minimum set of *nif* genes proposed by Dos Santos (7).  
623 Remarkably, the collection contained a mixture of diazotrophs that were categorized into three  
624 groups: the DSP group of diazotrophs fully adherent to the Dos Santos model for essential *nif*  
625 gene content, a smaller group of SDS diazotrophs with incomplete versions of the Dos Santos  
626 model, and the DSN group that completely lacked all six essential *nif* genes (Fig 3, S3 Fig, S4  
627 Fig and S5 Fig). While the DSP group consisted of diazotrophs that possessed homologous  
628 sequences to HMMs for all six essential *nif* genes (*nif*HDKENB) of the Dos Santos model along  
629 with matches to the majority of other NIF regulon genes (7), discovery of the DSN and SDS  
630 isolates lacking homologous sequences to this set of canonical *nif* genes either entirely, or in-  
631 part, was unexpected. Interestingly, absence of matches to the HMM for the *nif*L gene that  
632 confers repression of the *nif*-specific transcriptional activator NifA in a large number of DSP  
633 diazotroph genomes suggests that these isolates may be acclimatized to high frequencies of  
634 nitrogen-fixing conditions in their native environment (58). Furthermore, the *nif*W gene was  
635 found to be non-essential for a large number of DSP diazotrophs that lacked presence of a  
636 homologous gene in their genome, which is corroborated by a previous report in *nif*W strains of  
637 *K. pneumoniae* (59). However, observations that all confirmed diazotrophs in the DSP group  
638 were adherent to the the well established genetic structure of the *K. pneumoniae* NIF regulon  
639 (44), and that genomes classified as *Klebsiella* were only assigned to the DSP group validated  
640 use of the *Klebsiella* model to examine the diazotrophic isolate genomes for canonical *nif* genes.

641 Taxonomic classification of diazotrophic genomes revealed a spectrum of phylogenetic  
642 diversity that was not found to be indicative of *nif* gene presence. For example, while  
643 gammaproteobacterial genera classified among DSP genomes included *Enterobacter*, *Klebsiella*,  
644 *Kosakonia*, *Metakosakonia*, *Pseudomonas*, *Rahnella* and *Raoultella*, the SDS and DSN groups  
645 contained genomes that were classified as *Enterobacter*, *Metakosakonia*, *Pseudomonas* and/or  
646 *Rahnella* as well. Our discovery of diazotrophs in the DSP group classified as  
647 Gammaproteobacteria suggested that bacteria of this taxonomic class from the mucilage  
648 environment are likely to contribute to the BNF phenotype of Sierra Mixe maize. This is  
649 supported by previous studies describing species from enterobacterial genera classified among  
650 genomes in the DSP group (*Enterobacter*, *Klebsiella*, *Kosakonia*, *Rahnella*, and *Raoultella*) as  
651 diazotrophic endophytes associated with cereal crops such as sugarcane, rice, and maize (60-64).  
652 Recent reports demonstrated the successful engineering of a *Pseudomonas* strain capable of  
653 associating with wheat and maize as a diazotrophic endophyte (65), as well as successful growth  
654 promotion of maize using a diazotrophic strain of *Pseudomonas* isolated from the rhizosphere of  
655 rice (66). However, to the best of our knowledge, a naturally occurring diazotrophic  
656 pseudomonad associated with maize endophytically is yet to be reported. Additionally, genomes  
657 in the SDS and DSN NIF groups were classified to many other genera outside of  
658 Gammaproteobacteria, which indicates that diazotrophs of Sierra Mixe maize exhibit much  
659 broader phylogenetic diversity relative to these previous reports of diazotrophs that associate  
660 with cereal crops.

661 **Many diazotrophs exhibited high BNF ratios independent of possessing canonical *nif* genes**

662 In contrast to our hypothesis, results from the BNF assay and *nif* gene mining confirmed a  
663 substantial portion of the isoated diazotrophs lacked homologous protein coding sequences to

664 many, or all, canonical *nif* genes of the Dos Santos and *Klebsiella* models yet exhibited high  
665 BNF ratios independent of canonical *nif* genes. Our quantitative assay to detect the incorporation  
666 of <sup>15</sup>N-dinitrogen from an enriched atmosphere into secreted metabolites served as a robust  
667 alternative to conventional methods of diazotrophic detection, such as colorimetric assays for  
668 ammonium secretion and the acetylene reduction assay, which limit detection of evidence for  
669 BNF to ammonium accumulation or secondary nitrogenase activity (i.e. production of ethylene  
670 through the reduction of acetylene gas), respectively (67, 68). As there has never been a  
671 documented case of diazotrophs utilizing atmospheric nitrogen without key components of the  
672 nitrogenase enzyme complex, our observations that SDS and DSN diazotrophs lacked protein  
673 coding sequences homologous to essential *nif* genes in their genomes (S4 Fig, S5 Fig) lead us to  
674 question the metabolic mechanisms that allowed them to be successfully cultured and isolated on  
675 nitrogen-free medium in the laboratory.

676         While comparison of *nif* gene profiles (Fig 3) with results from the BNF assay confirmed  
677 that DSP isolates utilize atmospheric nitrogen for growth, comparison with BNF assay results for  
678 the SDS and DSN NIF groups indicated that these isolates were also capable of incorporating  
679 atmospheric nitrogen into secreted metabolites at efficiencies that both rivaled and exceeded  
680 those of DSP isolates in some cases (Fig 4). For example, while lactococci are commonly  
681 associated with plants (69), our investigation serves as the first report of diazotrophic lactococci  
682 based on observations that *Lactococcus* isolates exhibited some of the highest BNF ratios (Fig  
683 4C, S2 Table). These results were unexpected due to the total absence of homologous sequences  
684 to HMMS for essential *nif* genes within lactococcal isolate genomes (Fig 3, S5 Fig), and  
685 suggested that bacteria of the mucilage microbiota lacking essential *nif* genes are capable of  
686 incorporating atmospheric nitrogen into their metabolism under N-limiting environmental

687 conditions through metabolic mechanisms outside of the Dos Santos and *Klebsiella* models.  
688 Taken together, the genome analysis and BNF assay results revealed that possession of canonical  
689 *nif* genes comprising the Dos Santos and *Klebsiella* models were not required for all diazotrophs  
690 from Sierra Mixe maize to exhibit BNF activity, suggesting that novel diazotrophic mechanisms  
691 exist in this community.

692         Uncovering the genetic underpinnings of the observed BNF phenotype for mucilage  
693 diazotrophs lacking canonical *nif* genes will rely on advances in genomic analysis and future  
694 experimentation. While HMMs derived from consensus sequences of full-length coding  
695 sequences serve as a reliable tool to detect known genomic features in bacteria, they do not invite  
696 the possibility of detecting novel protein coding sequences conferring known biological  
697 functions through alternative protein domain architecture. Therefore, advances in genome  
698 annotation that integrate machine learning algorithms with HMM libraries derived from  
699 consensus sequences of protein domains rather than full-length coding sequences, such as  
700 *Nanotext*, may enable the discovery of new proteins conferring familiar activities (70).  
701 Additionally, implementation of microbial pan-genome association studies using appropriate  
702 control groups for DSN isolates with confirmed BNF phenotypes may also shed light on  
703 additional significant genes associated with diazotrophy (71).

#### 704 **Alternative nitrogenase genes were not present in SDS and DSN isolate genomes**

705 We queried WGS from diazotrophic isolates for protein coding sequences homologous to known  
706 alternative nitrogenase genes in search of an explanation for the discovery that confirmed  
707 diazotrophic isolates lacked essential *nif* genes of the Dos Santos and *Klebsiella* models.  
708 Environments with limited abundance of molybdenum often harbor diazotrophic bacteria that  
709 exhibit genetic operons encoding alternative nitrogenase systems. These include Vanadium-Iron



710 (Vn-Fe) type and Iron-only type nitrogenases (Fe-Fe) that assume quaternary structure without  
711 utilization of molybdenum and the assistance of an additional *nif* gene encoding the *gamma*  
712 subunit for the catalytic component (43). Additionally, these operons arose over evolutionary  
713 time through genetic duplication events and neofunctionalization of the Fe-Mo *nif*HDK operon  
714 in response to abiotic stress (43, 53). Referencing previous reports on the nutrient deficient  
715 quality of indigenous fields for Sierra Mixe maize cultivation (6), the BNF assay, and *nif* gene  
716 mining results, we hypothesized that SDS and DSN diazotrophs possessed alternative *nif* genes  
717 and tested it by scanning the protein coding sequences of diazotroph genomes with HMMs for  
718 the Vn-Fe *nif* genes (*vnf*) and Fe-Fe *nif* genes (*anf*).

719         While results from this investigation forced the rejection of our hypothesis by confirming  
720 that SDS and DSN isolates do not possess alternative *nif* genes, they did reveal discovery of a  
721 subset of diazotrophs from the DSP group that possessed genes resembling the *anf* and *vnf*  
722 genetic operons. We found 42 diazotrophs with genes matching TIGRFAMs from all three  
723 classes of known nitrogenase systems (Fig 5A). Although unexpected, this result corroborates  
724 the previous report that alternative *nif* genes were only found to occur in diazotrophs that also  
725 possessed the Mo-Fe nitrogenase system (53), and the observation of alternative *nif* gene  
726 sequences in Sierra Mixe mucilage (6).

727         Comparison of whole genome nucleotide composition for diazotrophs with homologs to  
728 alternative *nif* genes provided evidence that this subset of the DSP NIF group exhibited  
729 considerable genomic diversity and contained distinct members with resemblance to previously  
730 reported *Metakosakonia* and *Raoultella* reference genomes (Fig 5B). However, this subset of  
731 diazotrophic isolates exhibited high genome dissimilarity and the group was found to contain  
732 genomes for which assignment to a known genus was unattainable through LCA classification

733 using the GTDB. These observations suggested that the mucilage microbiota harbors  
734 *Metakosakonia* and *Raoultella* with alternative *nif* genes and variation in metabolic capabilities,  
735 as well as potentially novel genera with considerable genomic differences. Further investigation  
736 by pan-genome analysis revealed large blocks of genomic features corresponding to the variation  
737 in genome composition observed in four isolate genomes that formed a distinct clade (Fig 5C).  
738 To our knowledge, this is the first report of maize-associated *Raoultella* exhibiting alternative *nif*  
739 genes, and the genomic evidence surrounding this discovery invites the possibility for  
740 classification of a new species within the genus.

741 This work reaffirmed the proposal of Sierra Mixe maize as a model system to investigate  
742 nitrogen fixation in cereal crops by validating its association with diazotrophic bacteria that  
743 possess canonical genetic operons for nitrogen fixation (72). Our investigation emphasized the  
744 importance of aerial root mucilage to the nitrogen-fixing phenotype of the system by confirming  
745 the presence of classical nitrogen fixing bacteria in the aerial root mucilage microbiota that  
746 contained the genomic potential to derive energy for BNF from mucilage polysaccharide. We  
747 also demonstrated that mucilage-derived diazotrophs incorporated atmospheric nitrogen into  
748 their metabolism through unknown metabolic pathways extending beyond current knowledge  
749 that defines BNF as bacterial conversion of dinitrogen to ammonia through the expression of  
750 canonical *nif* gene products within the Dos Santos and *Klebsiella* models. We succeeded in  
751 recovering and characterizing diazotrophs from the mucilage microbiota and found diazotrophs  
752 that did not contain any canonical *nif* genes, suggesting their use of novel genes for the  
753 conversion of dinitrogen into organic nitrogen forms that were assimilated into many small  
754 molecules exported by the organisms. Collectively, this study demonstrated that specific

755 microbiome members of Sierra Mixe maize display diazotrophy with multiple molecular  
756 mechanisms.

## 757 **Funding information**

758 Mars, Incorporated <http://www.mars.com/global>. The research was funded by an unrestricted gift  
759 and a grant to ABB and BCW. The funder had no role in study design, data collection and  
760 analysis, decision to publish, or preparation of the manuscript. The research was funded by  
761 grants to ABB from BioN2, Incorporated. The funder had no role in study design, data collection  
762 and analysis, decision to publish, or preparation of the manuscript. The research was also funded  
763 by United States Department of Agriculture (USDA) by a grant to BCW (award #2019-67013-  
764 29724).

765

## 766 **Author Contributions**

767 BCW and MY and NK carried out the strategy to culture, isolate and store the microbial  
768 collection from Sierra Mixe maize. SMH, TP and BH constructed DNA sequencing libraries for  
769 WGS of bacterial isolates and BH conducted the genome sequencing. SMH carried out all  
770 bioinformatic analyses related to WGS analysis with guidance from BCW and CTB. BCW and  
771 RJ designed the BNF assay, established the method and analyzed the associated data, and NK  
772 conducted the experiments. SMH wrote the first draft of the manuscript. ABB, BCW, CTB,  
773 SMH and TP edited and revised the manuscript.

## 774 **Conflict of interest**

775 The authors declare no conflicts of interests. None of the authors are employed by the major  
776 funding agency of this work, MARS, Inc.

## 777 **References**

- 778 1. Rosenblueth M, Ormeño-Orrillo E, López-López A, Rogel MA, Reyes-Hernández BJ,  
779 Martínez-Romero JC, et al. Nitrogen Fixation in Cereals. *Frontiers in Microbiology*.  
780 2018;9(1794).
- 781 2. Giller KE. Nitrogen fixation in tropical cropping systems: CABI; 2001.
- 782 3. Yusuf AA, Iwuafor ENO, Abaidoo RC, Olufajo OO, Sanginga N. Grain legume rotation  
783 benefits to maize in the northern Guinea savanna of Nigeria: fixed-nitrogen versus other  
784 rotation effects. *Nutrient Cycling in Agroecosystems*. 2009;84(2):129-39.
- 785 4. Triplett EW. Diazotrophic endophytes: progress and prospects for nitrogen fixation in  
786 monocots. *Plant and Soil*. 1996;186(1):29-38.
- 787 5. Philippot L, Raaijmakers JM, Lemanceau P, Van Der Putten WH. Going back to the roots:  
788 the microbial ecology of the rhizosphere. *Nature Reviews Microbiology*. 2013;11(11):789.
- 789 6. Van Deynze A, Zamora P, Delaux P-M, Heitmann C, Jayaraman D, Rajasekar S, et al.  
790 Nitrogen fixation in a landrace of maize is supported by a mucilage-associated diazotrophic  
791 microbiota. *PLoS biology*. 2018;16(8):e2006352.
- 792 7. Dos Santos PC, Fang Z, Mason SW, Setubal JC, Dixon R. Distribution of nitrogen fixation  
793 and nitrogenase-like sequences amongst microbial genomes. *BMC Genomics*.  
794 2012;13(1):162-.

- 795 8. Villas - Bôas SG, Højer - Pedersen J, Åkesson M, Smedsgaard J, Nielsen J. Global  
796 metabolite analysis of yeast: evaluation of sample preparation methods. *Yeast*.  
797 2005;22(14):1155-69.
- 798 9. Xie Y, Chou LS, Cutler A, Weimer B. DNA macroarray profiling of *Lactococcus lactis*  
799 subsp *lactis* IL1403 gene expression during environmental stresses. *Applied and*  
800 *Environmental Microbiology*. 2004;70(11):6738-47.
- 801 10. Draper JL, Hansen LM, Bernick DL, Abedrabbo S, Underwood JG, Kong N, et al. Fallacy  
802 of the Unique Genome: Sequence Diversity within Single *Helicobacter pylori* Strains.  
803 *MBio*. 2017;8(1).
- 804 11. Xia JG, Sinelnikov IV, Han B, Wishart DS. MetaboAnalyst 3.0-making metabolomics more  
805 meaningful. *Nucleic Acids Research*. 2015;43(W1):W251-W7.
- 806 12. Bolger AM, Lohse M, Usadel B. Trimmomatic: a flexible trimmer for Illumina sequence  
807 data. *Bioinformatics*. 2014:btu170.
- 808 13. Li D, Liu C-M, Luo R, Sadakane K, Lam T-W. MEGAHIT: an ultra-fast single-node  
809 solution for large and complex metagenomics assembly via succinct de Bruijn graph.  
810 *Bioinformatics*. 2015:btv033.
- 811 14. Gurevich A, Saveliev V, Vyahhi N, Tesler G. QUAST: quality assessment tool for genome  
812 assemblies. *Bioinformatics*. 2013;29(8):1072-5.
- 813 15. Kang DD, Froula J, Egan R, Wang Z. MetaBAT, an efficient tool for accurately  
814 reconstructing single genomes from complex microbial communities. *PeerJ*. 2015;3:e1165.
- 815 16. Li H, Handsaker B, Wysoker A, Fennell T, Ruan J, Homer N, et al. The sequence  
816 alignment/map format and SAMtools. *Bioinformatics*. 2009;25(16):2078-9.
- 817 17. Li H, Durbin R. Fast and accurate short read alignment with Burrows–Wheeler transform.  
818 *bioinformatics*. 2009;25(14):1754-60.

- 819 18. Brown CT, Irber L. sourmash: a library for MinHash sketching of DNA. *J Open Source*  
820 *Software*. 2016;1(5):27.
- 821 19. Ondov BD, Treangen TJ, Melsted P, Mallonee AB, Bergman NH, Koren S, et al. Mash: fast  
822 genome and metagenome distance estimation using MinHash. *Genome Biol*.  
823 2016;17(1):132.
- 824 20. Wood DE, Salzberg SL. Kraken: ultrafast metagenomic sequence classification using exact  
825 alignments. *Genome Biol*. 2014;15(3):R46.
- 826 21. Gu Z, Eils R, Schlesner MJB. Complex heatmaps reveal patterns and correlations in  
827 multidimensional genomic data. 2016;32(18):2847-9.
- 828 22. Foster ZS, Sharpton TJ, Grünwald NJ. Metacoder: An R package for visualization and  
829 manipulation of community taxonomic diversity data. *PLoS computational biology*.  
830 2017;13(2):e1005404.
- 831 23. Wood DE, Lu J, Langmead B. Improved metagenomic analysis with Kraken 2. *Genome*  
832 *biology*. 2019;20(1):257.
- 833 24. Pruitt KD, Tatusova T, Maglott DR. NCBI reference sequences (RefSeq): a curated non-  
834 redundant sequence database of genomes, transcripts and proteins. *Nucleic acids research*.  
835 2007;35(suppl\_1):D61-D5.
- 836 25. Foster ZS, Sharpton TJ, Grunwald NJ. Metacoder: An R package for visualization and  
837 manipulation of community taxonomic diversity data. *PLoS Comput Biol*.  
838 2017;13(2):e1005404.
- 839 26. Lu J, Breitwieser FP, Thielen P, Salzberg SL. Bracken: estimating species abundance in  
840 metagenomics data. *Peerj Computer Science*. 2017;3:e104.
- 841 27. McMurdie PJ, Holmes S. phyloseq: an R package for reproducible interactive analysis and  
842 graphics of microbiome census data. *PLoS One*. 2013;8(4):e61217.

- 843 28. Seemann T. Prokka: rapid prokaryotic genome annotation. *Bioinformatics*.  
844 2014;30(14):2068-9.
- 845 29. Eddy SR. HMMER: Profile hidden Markov models for biological sequence analysis. 2001.
- 846 30. Haft DH, Loftus BJ, Richardson DL, Yang F, Eisen JA, Paulsen IT, et al. TIGRFAMs: a  
847 protein family resource for the functional identification of proteins. *Nucleic acids research*.  
848 2001;29(1):41-3.
- 849 31. Bateman A, Coin L, Durbin R, Finn RD, Hollich V, Griffiths - Jones S, et al. The Pfam  
850 protein families database. *Nucleic acids research*. 2004;32(suppl\_1):D138-D41.
- 851 32. Wickham H, Francois R. dplyr: A grammar of data manipulation. R package version 04.  
852 2015;1:20.
- 853 33. Zhang H, Yohe T, Huang L, Entwistle S, Wu P, Yang Z, et al. dbCAN2: a meta server for  
854 automated carbohydrate-active enzyme annotation. *Nucleic Acids Res*. 2018;46(W1):W95-  
855 W101.
- 856 34. Wickham H, Averick M, Bryan J, Chang W, McGowan L, François R, et al. Welcome to the  
857 Tidyverse. *Journal of Open Source Software*. 2019;4(43):1686.
- 858 35. Yu G, Smith DK, Zhu H, Guan Y, Lam TT-Y. ggtree: an r package for visualization and  
859 annotation of phylogenetic trees with their covariates and other associated data. *Methods in*  
860 *Ecology and Evolution*. 2017;8(1):28-36.
- 861 36. Seemann T. Prokka: rapid prokaryotic genome annotation. *Bioinformatics*.  
862 2014;30(14):2068-9.
- 863 37. Page AJ, Cummins CA, Hunt M, Wong VK, Reuter S, Holden MT, et al. Roary: rapid large-  
864 scale prokaryote pan genome analysis. *Bioinformatics*. 2015;31(22):3691-3.
- 865 38. Hadfield J, Croucher NJ, Goater RJ, Abudahab K, Aanensen DM, Harris SR. Phandango: an  
866 interactive viewer for bacterial population genomics. *Bioinformatics*. 2017;34(2):292-3.

- 867 39. Carvalho TL, Balsemao-Pires E, Saraiva RM, Ferreira PC, Hemerly AS. Nitrogen signalling  
868 in plant interactions with associative and endophytic diazotrophic bacteria. *J Exp Bot.*  
869 2014;65(19):5631-42.
- 870 40. Amicucci MJ, Galermo AG, Guerrero A, Treves G, Nandita E, Kailemia MJ, et al. Strategy  
871 for Structural Elucidation of Polysaccharides: Elucidation of a Maize Mucilage that Harbors  
872 Diazotrophic Bacteria. *Anal Chem.* 2019;91(11):7254-65.
- 873 41. Cantarel BL, Coutinho PM, Rancurel C, Bernard T, Lombard V, Henrissat B. The  
874 Carbohydrate-Active EnZymes database (CAZy): an expert resource for Glycogenomics.  
875 *Nucleic Acids Res.* 2009;37(Database issue):D233-8.
- 876 42. Saier MH, Jr., Reddy VS, Tsu BV, Ahmed MS, Li C, Moreno-Hagelsieb G. The Transporter  
877 Classification Database (TCDB): recent advances. *Nucleic acids research.*  
878 2016;44(D1):D372-D9.
- 879 43. Mus F, Alleman AB, Pence N, Seefeldt LC, Peters JW. Exploring the alternatives of  
880 biological nitrogen fixation. *Metallomics.* 2018;10(4):523-38.
- 881 44. Arnold W, Rump A, Klipp W, Priefer UB, Pühler AJJomb. Nucleotide sequence of a  
882 24,206-base-pair DNA fragment carrying the entire nitrogen fixation gene cluster of  
883 *Klebsiella pneumoniae*. 1988;203(3):715-38.
- 884 45. Milenkov M, Thummer R, Glöer J, Grötzinger J, Jung S, Schmitz RA. Insights into  
885 membrane association of *Klebsiella pneumoniae* NifL under nitrogen-fixing conditions from  
886 mutational analysis. *Journal of bacteriology.* 2011;193(3):695-705.
- 887 46. Chaumeil P-A, Mussig AJ, Hugenholtz P, Parks DH. GTDB-Tk: a toolkit to classify  
888 genomes with the Genome Taxonomy Database. *Bioinformatics.* 2019.
- 889 47. Varghese NJ, Mukherjee S, Ivanova N, Konstantinidis KT, Mavrommatis K, Kyrpides NC,  
890 et al. Microbial species delineation using whole genome sequences. *Nucleic acids research.*  
891 2015:gkv657.



- 892 48. Jain C, Rodriguez-R LM, Phillippy AM, Konstantinidis KT, Aluru S. High throughput ANI  
893 analysis of 90K prokaryotic genomes reveals clear species boundaries. *Nature*  
894 *Communications*. 2018;9(1):5114.
- 895 49. Haiminen N, Edlund S, Chambliss D, Kunitomi M, Weimer BC, Ganesan B, et al. Food  
896 authentication from shotgun sequencing reads with an application on high protein powders.  
897 *NPJ science of food*. 2019;3(1):1-11.
- 898 50. Bulgarelli D, Schlaeppi K, Spaepen S, Van Themaat EVL, Schulze-Lefert P. Structure and  
899 functions of the bacterial microbiota of plants. *Annual review of plant biology*.  
900 2013;64:807-38.
- 901 51. Hardoim P, Nissinen R, van Elsas JD. Ecology of bacterial endophytes in sustainable  
902 agriculture. *Bacteria in Agrobiolology: Plant Probiotics*: Springer; 2012. p. 97-126.
- 903 52. Levy A, Gonzalez IS, Mittelviefhaus M, Clingenpeel S, Paredes SH, Miao JM, et al.  
904 Genomic features of bacterial adaptation to plants. *Nature Genetics*. 2018;50(1):138-150.
- 905 53. Raymond J, Siefert JL, Staples CR, Blankenship RE. The natural history of nitrogen  
906 fixation. *Molecular biology and evolution*. 2004;21(3):541-54.
- 907 54. Amicucci MJ, Galermo AG, Guerrero A, Treves G, Nandita E, Kailemia MJ, et al. Strategy  
908 for Structural Elucidation of Polysaccharides: Elucidation of a Maize Mucilage that Harbors  
909 Diazotrophic Bacteria. *Analytical Chemistry*. 2019.
- 910 55. Pozzo T, Higdon SM, Pattathil S, Hahn MG, Bennett AB. Characterization of novel  
911 glycosyl hydrolases discovered by cell wall glycan directed monoclonal antibody screening  
912 and metagenome analysis of maize aerial root mucilage. *PloS one*. 2018;13(9):e0204525.
- 913 56. Cantarel BL, Coutinho PM, Rancurel C, Bernard T, Lombard V, Henrissat B. The  
914 Carbohydrate-Active EnZymes database (CAZy): an expert resource for Glycogenomics.  
915 *Nucleic Acids Research*. 2008;37(suppl\_1):D233-D8.
- 916 57. Saier Jr MH. Families of transmembrane sugar transport proteins: MicroReview. *Molecular*  
917 *microbiology*. 2000;35(4):699-710.

- 918 58. Milenkov M, Thummer R, Gloer J, Grotzinger J, Jung S, Schmitz RA. Insights into  
919 Membrane Association of *Klebsiella pneumoniae* NifL under Nitrogen-Fixing Conditions  
920 from Mutational Analysis. *Journal of Bacteriology*. 2011;193(3):695-705.
- 921 59. PAUL W, MERRICK M. The roles of the *nifW*, *nifZ* and *nifM* genes of *Klebsiella*  
922 *pneumoniae* in nitrogenase biosynthesis. *European journal of biochemistry*.  
923 1989;178(3):675-82.
- 924 60. Chen M, Zhu B, Lin L, Yang L, Li Y, An Q. Complete genome sequence of *Kosakonia*  
925 *sacchari* type strain SP1(T.). *Standards in genomic sciences*. 2014;9(3):1311-8.
- 926 61. Govindarajan M, Kwon S-W, Weon H-Y. Isolation, molecular characterization and growth-  
927 promoting activities of endophytic sugarcane diazotroph *Klebsiella* sp. GR9. *World Journal*  
928 *of Microbiology and Biotechnology*. 2007;23(7):997-1006.
- 929 62. Andreozzi A, Prieto P, Mercado-Blanco J, Monaco S, Zampieri E, Romano S, et al.  
930 Efficient colonization of the endophytes *Herbaspirillum huttiense* RCA24 and *Enterobacter*  
931 *cloacae* RCA25 influences the physiological parameters of *Oryza sativa* L. cv. Baldo rice.  
932 *Environmental Microbiology*. 2019;21(9):3489-504.
- 933 63. Kandel SL, Joubert PM, Doty SL. Bacterial Endophyte Colonization and Distribution within  
934 Plants. *Microorganisms*. 2017;5(4):77.
- 935 64. Luo T, Ou - Yang XQ, Yang LT, Li YR, Song XP, Zhang GM, et al. *Raoultella* sp. strain  
936 L03 fixes N<sub>2</sub> in association with micropropagated sugarcane plants. *Journal of basic*  
937 *microbiology*. 2016;56(8):934-40.
- 938 65. Fox AR, Soto G, Valverde C, Russo D, Lagares Jr A, Zorreguieta Á, et al. Major cereal  
939 crops benefit from biological nitrogen fixation when inoculated with the nitrogen-fixing  
940 bacterium *Pseudomonas protegens* Pf-5 X940. *Environmental Microbiology*.  
941 2016;18(10):3522-34.

- 942 66. Ke X, Feng S, Wang J, Lu W, Zhang W, Chen M, et al. Effect of inoculation with nitrogen-  
943 fixing bacterium *Pseudomonas stutzeri* A1501 on maize plant growth and the microbiome  
944 indigenous to the rhizosphere. *Syst Appl Microbiol*. 2019;42(2):248-60.
- 945 67. Hardy RWF, Burns RC, Holsten RD. Applications of the acetylene-ethylene assay for  
946 measurement of nitrogen fixation. *Soil Biology and Biochemistry*. 1973;5(1):47-81.
- 947 68. Shand CA, Williams BL, Coutts G. Determination of N-species in soil extracts using  
948 microplate techniques. *Talanta*. 2008;74(4):648-54.
- 949 69. Song AA-L, In LLA, Lim SHE, Rahim RA. A review on *Lactococcus lactis*: from food to  
950 factory. *Microbial cell factories*. 2017;16(1):55-.
- 951 70. Viehweger A, Krautwurst S, König B, Marz M. Distributed representations of protein  
952 domains and genomes and their compositionality. *bioRxiv*. 2019:524280.
- 953 71. Brynildsrud O, Bohlin J, Scheffer L, Eldholm V. Rapid scoring of genes in microbial pan-  
954 genome-wide association studies with Scoary. *Genome Biology*. 2016;17(1):238.
- 955 72. Bennett AB, Pankiewicz VCS, Ané J-M. A Model for Nitrogen Fixation in Cereal Crops.  
956 *Trends in Plant Science*. 2020.
- 957 73. Hadfield J, Croucher NJ, Goater RJ, Abudahab K, Aanensen DM, Harris SR. Phandango: an  
958 interactive viewer for bacterial population genomics. *Bioinformatics*. 2018;34(2):292-3.
- 959
- 960

961 **List of Tables**

962 **Table 1. Summary of BNF Assay Results.** Isolates were grouped using defined ranges of  
963  $^{15}\text{N}/^{14}\text{N}$  ratio values.  $^{15}\text{N}/^{14}\text{N}$  ratios were computed by summing the peak intensities of all N-  
964 containing bio-markers common to both enriched and control cultures that had q-values less than  
965 or equal to 0.05 after analyzing metabolite data using Metaboanalyst (11).

<b>BNF Group</b>	<b>N Isolates</b>	<b><math>^{15}\text{N}/^{14}\text{N}</math> Ratio</b>
A	4	$x > 4$
B	10	$4 > x > 3$
C	14	$3 > x > 2$
D	461	$2 > x > 1$
E	85	$x < 1$
F	14	Not determined

966

967

## 968 **List of Figures**

### 969 **Fig 1. Comparative analysis of draft genome assemblies from Sierra Mixe bacterial isolates.**

970 All-by-all comparison of MinHash sketches of draft genome assemblies from 588 bacterial  
971 isolates using Sourmash (18) . MinHash sketches of each draft genome assembly used in the  
972 comparison had a k-mer size of 31. Genus classification from MinHash sketches for each isolate  
973 genome is presented as a color-coded sidebar alongside the matrix. Results from genome binning  
974 analysis with Metabat (15) is included as a second color-coded sidebar. The Jaccard Index scale  
975 represents the Jaccard Similarity Index (JSI) value computed for each pairwise comparison of  
976 isolate genome MinHash sketches. Darker coloring indicates higher genome similarity and  
977 lighter coloring indicates lower similarity.

978

### 979 **Fig 2. Glycosyl hydrolase and sugar transporter genome profiles of diazotrophic isolates.**

980 Analysis using dbCAN2 (33) was done to query total predicted coding sequences in each  
981 genome. Gene sequences encoding CAZymes and sugar transporters with substrate specificities  
982 that correspond to monosaccharide residues of the Sierra Mixe aerial root mucilage  
983 polysaccharide were selected from query results by generating a manually curated list of CAZY  
984 HMMs and TCDB accession IDs. Predicted gene sequence-HMM matching pairs were reported  
985 after filtering total hits from each genome to select all records with > 85% model coverage and  
986 an e-value  $\leq 1e^{-09}$ . A) Glycosyl Hydrolase family HMM hits with designated sugar residue  
987 specificities: Ara – Arabinose, Gal – Galactose, GlcA – Glucuronic Acid, Fuc – Fucose, Man –  
988 Mannose, Xyl – Xylose. B) Sugar Transporter HMM-Gene hits with designated sugar residue  
989 transporter activity.

990 **Fig 3. Canonical *nif* gene profiles of diazotrophic isolate genomes.** Total predicted protein  
991 sequences of each pure isolate genome were queried against Hidden Markov Models (HMMs)  
992 for genes of the *K. pneumoniae* NIF regulon – including the six essential *nif* genes of the Dos  
993 Santos (DS) Model. Pure isolate genomes were clustered based on their relative MinHash  
994 genomic distances followed by heatmap visualization of their associated *nif* gene profiles. Three  
995 groups of pure diazotrophic isolates were formed based on the detected presence of homologous  
996 protein coding sequences to *nif*HDKENB: DS-Positive (DSP; red), Semi-DS (SDS; green) and  
997 DS-Negative (DSN; blue). Predicted amino acid sequence queries for each genome were  
998 considered as matches if *nif* gene HMM coverage was greater than or equal to 75% along with e-  
999 values  $\leq 1e^{-9}$ .

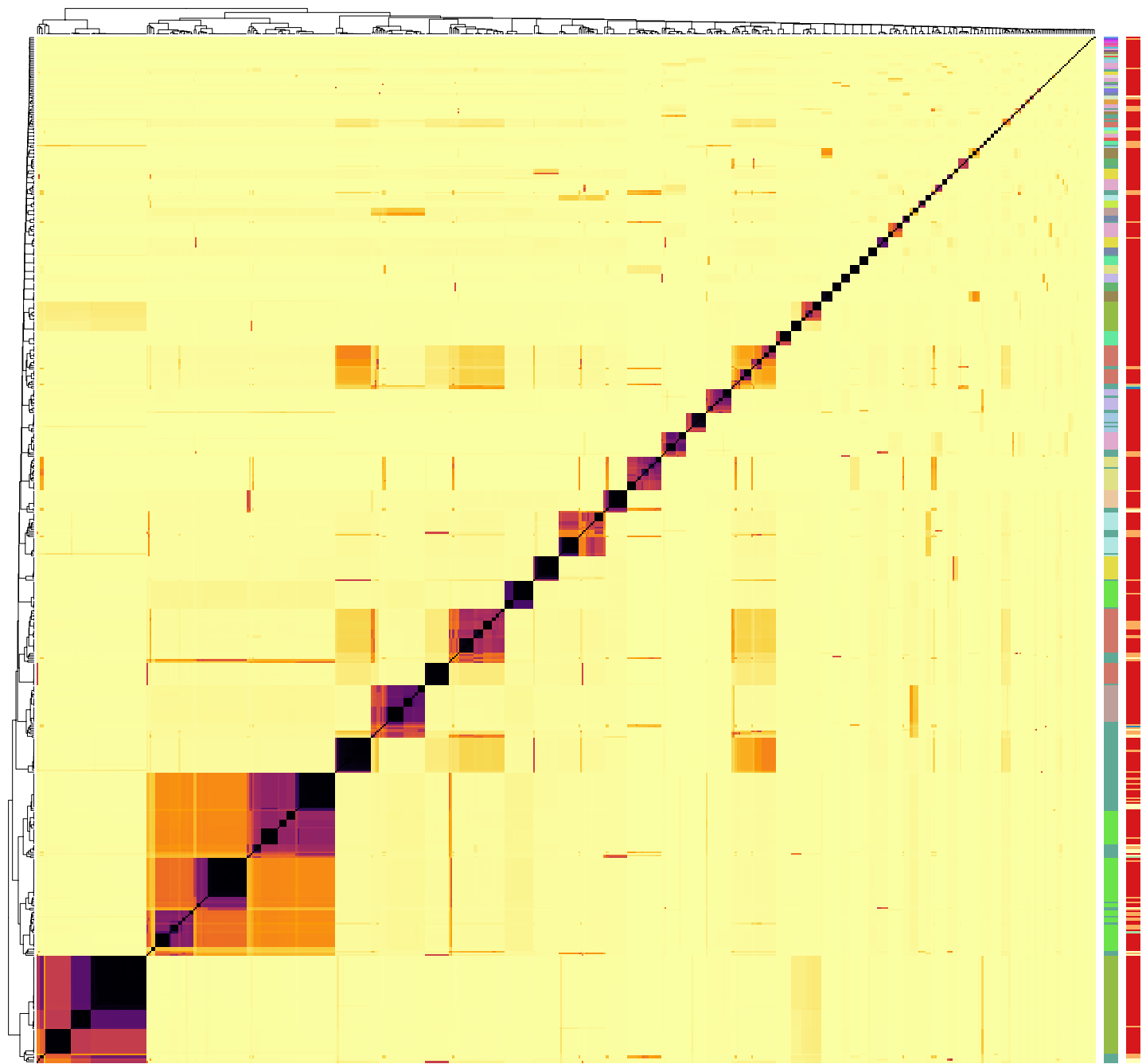
1000

1001 **Fig 4. BNF ratios of mucilage diazotrophs from atmospheric  $^{15}\text{N}_2$  incorporation assay.** As a  
1002 means to connect each diazotroph's *nif* gene profile with its corresponding BNF phenotype, BNF  
1003 ratios are presented in heatmaps that accompany dendrograms clustered by MinHash genome  
1004 distance under the context of the three NIF Groups determined from the genome mining analysis  
1005 (Fig 3). Heatmap annotations indicate the  $^{15}\text{N}/^{14}\text{N}$  ratios (BNF ratios) that represent the  
1006 summation of peak intensities for all N-containing metabolites used as biomarkers in the assay.  
1007 A) Dos-Santos Positive (DSP) isolates; B) Semi-Dos Santos (SDS) isolates; C) Dos-Santos  
1008 Negative (DSN) isolates. Grey bars on the BNF ratio heatmap indicate values that were not  
1009 determined.

1010

1011 **Fig 5. Mucilage bacterial isolates exhibit alternative nitrogenase genes.** A) The presence of  
1012 predicted protein sequences in diazotrophic isolate genomes was detected using TIGRFAM

1013 HMMs corresponding to the Fe-Fe and Vn-Fe alternative *nif* genes (*anfD*, *anfK*, *anfG*, *vnfD*,  
1014 *vnfK*, *vnfG*) along with HMMs for *nifHDK*. Genomes with detected presence of the targeted  
1015 genes were compared and quantified using a Venn Diagram to determine the list of diazotrophs  
1016 with genes resembling Vn-Fe, Fe-Only, Mo-Fe Type nitrogenases and *nifH*. B) Genomes with  
1017 alternative *nif* genes were compared using Sourmash and visualized as a composite matrix that  
1018 included annotation of genus level classification. C) Pan-genome analysis of diazotrophs with  
1019 alternative *nif* genes was conducted using Roary (37) and data for gene presence and absence  
1020 was visualized using Phandango (73) along with genus classification data from Sourmash LCA.  
1021 Orange annotations indicate genomes classified as *Metakosakonia*, green annotations indicate  
1022 *Raoultella* isolates, and purple annotations indicate “unassigned” classification at the genus  
1023 level.



Jaccard Index

0 0.2 0.4 0.6 0.8 1

Genus

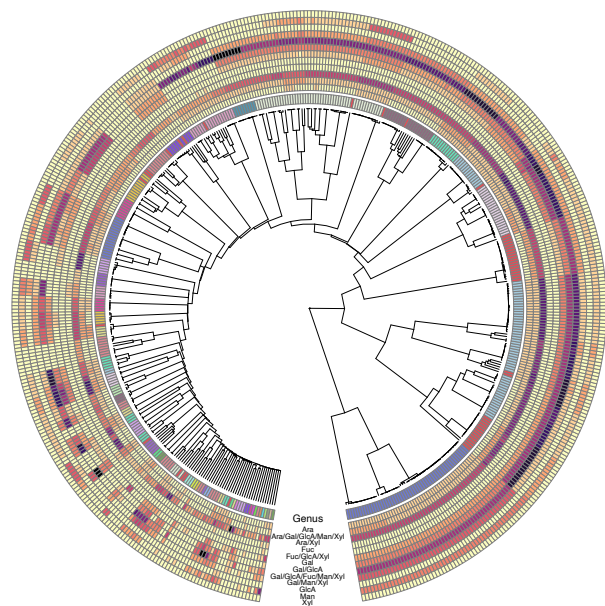
Achromobacter	Atlantibacter	Curtobacterium	Escherichia	Kosakonia	Lelliottia	Morganella	Raoultella	Stenotrophomonas
Acidovorax	Bacillus	Enterobacter	Hafnia	Lactococcus	Metakosakonia	Pantoea	Rhodococcus	unassigned
Acinetobacter	Burkholderia	Enterococcus	Herbaspirillum	Leclercia	Microbacterium	Pseudomonas	Serratia	
Agrobacterium	Citrobacter	Erwinia	Klebsiella	Leifsonia	Micrococcus	Rahnella	Staphylococcus	

N Bins

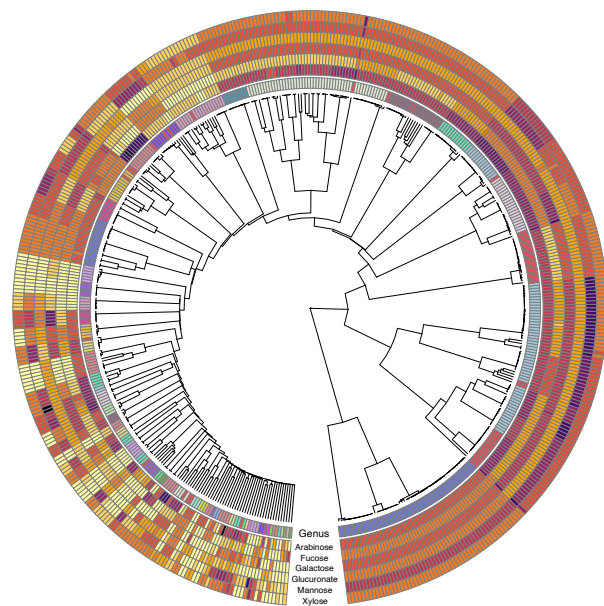
1  
2  
3  
4  
5



A



B



Glycosyl Hydrolase HMM Hits



Acidovorax  
Acinetobacter  
Agrobacterium  
Atlantibacter  
Bacillus  
Citrobacter  
Curtobacterium  
Enterobacter  
Erwinia  
Escherichia

Hafnia  
Herbaspirillum  
Klebsiella  
Kosakonia  
Lactococcus

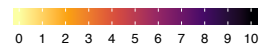
Genus

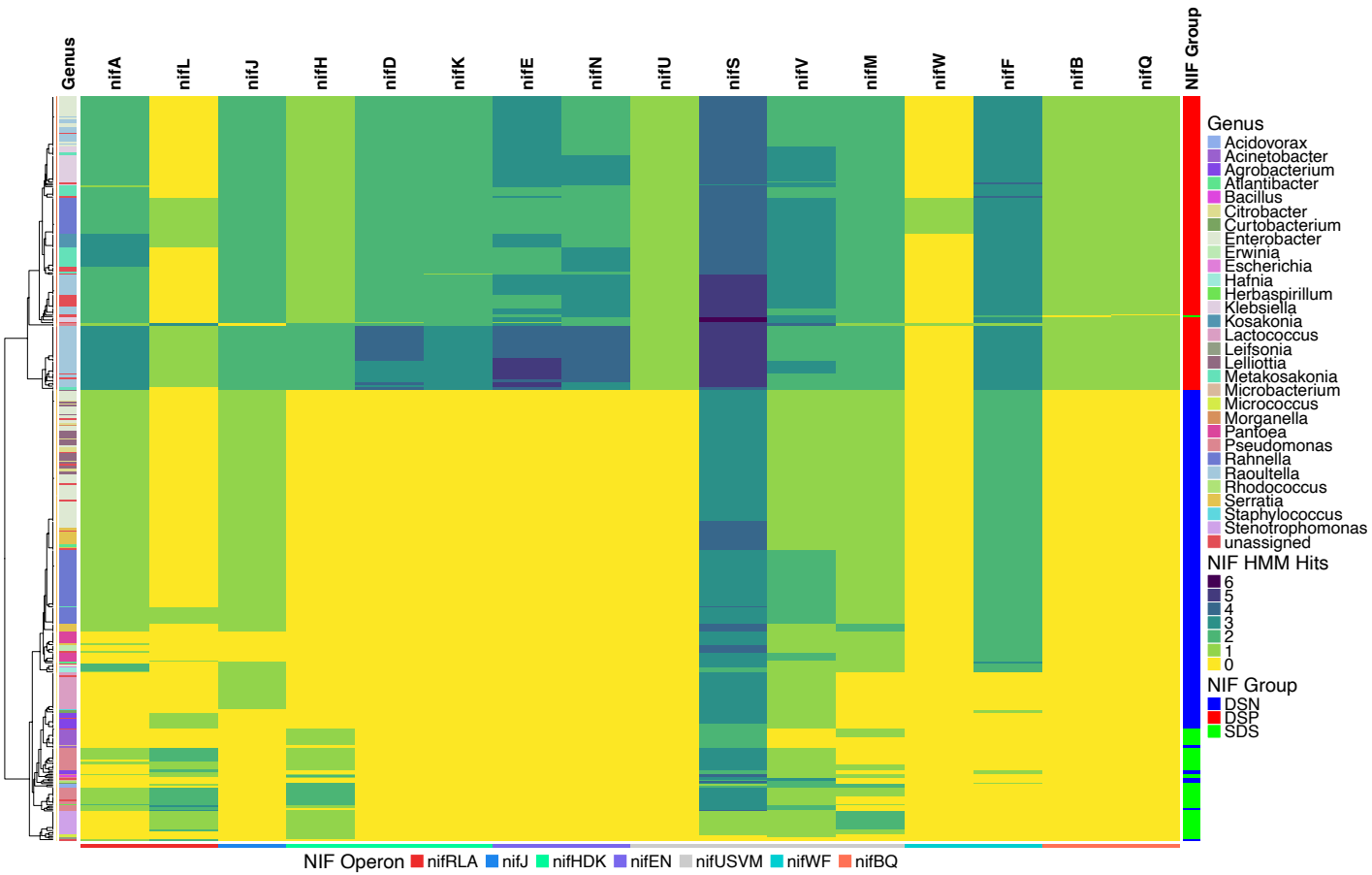
Leifsonia  
Lelliottia  
Metakosakonia  
Microbacterium  
Micrococcus

Morganella  
Parvooia  
Pseudomonas  
Rahnella  
Raoultella

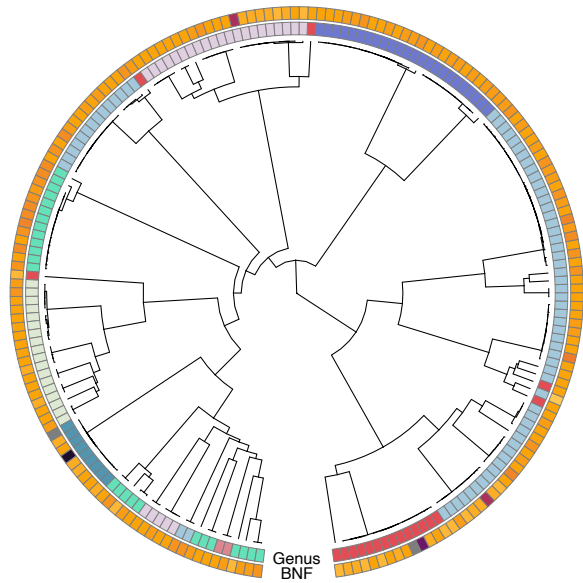
Rhodococcus  
Serratia  
Staphylococcus  
Stenotrophomonas  
unassigned

TCDB Diamond Hits

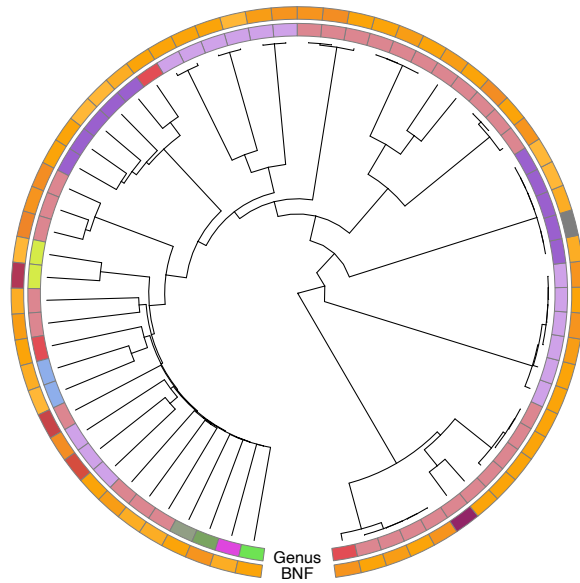




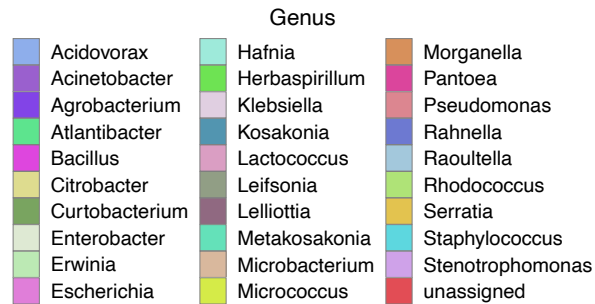
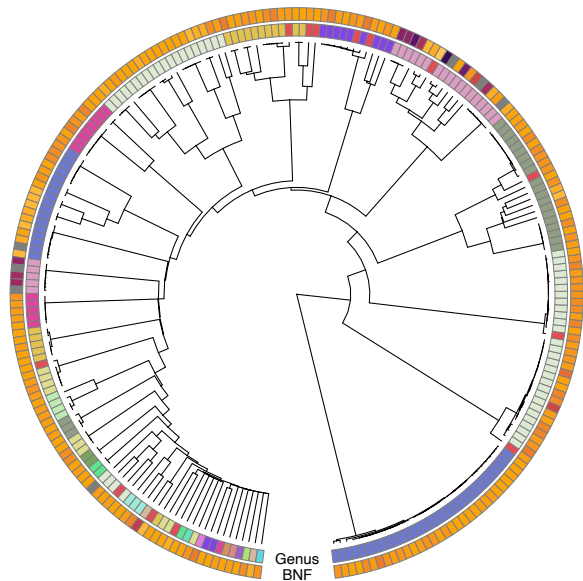
A



B



C



BNF (15N/14N Ratio)

